2010

DRUG RELEASE AND PHARMACOKINETIC PROPERTIES OF LIPOSOMAL DB-67

Yali Liang
University of Kentucky, ylian2@uky.edu

ABSTRACT OF THESIS

DRUG RELEASE AND PHARMACOKINETIC PROPERTIES OF LIPOSOMAL DB-67

Sterically stabilized liposomes with saturated lipid as the major lipid component (DSPC:m-PEG-DSPE 95:5 mole%) were applied in DB-67 delivery. The drug retention *in vitro* and pharmacokinetic properties *in vivo* were investigated. Liposomal DB-67 was cleared faster from the circulation in the larger liposomes (~180 nm) than in the smaller ones (~120 nm), even though DB-67 was retained longer in smaller size liposomes *in vitro*. Liposomal DB-67 clearance was increased when cholesterol was present in the liposomal composition (40 mole %). It can be attributable to the faster drug release from cholesterol containing liposomes as compared to liposomes without cholesterol. Cholesterol free liposomes with smaller particle size (~120 nm) were chosen as the optimal formulation. In addition, high lipid doses led to the lower clearance of liposomal DB-67 because the liposomal carriers were retained in the circulation longer. Liposomes of larger particle size were taken up by the liver and spleen to a greater extent than the smaller ones. But cholesterol content and lipid dose did not alter the tissue uptake of liposomes. The area under the DB-67 plasma concentration-time curve (AUC) for liposomal DB-67 was 40-fold higher that for non-liposomal DB-67.

KEYWORDS: Liposomes; DB-67; Pharmacokinetics; Cholesterol; Biodistribution

Yali Liang

08/02/2010

DRUG RELEASE AND PHARMACOKINETIC PROPERTIES OF LIPOSOMAL DB-67

By

Yali Liang

Dr. Markos Leggas

Director of Thesis

Dr. Jim Pauly

Director of Graduate Studies

08/02/2010

RULES FOR THE USE OF THESES

Unpublished theses submitted for the Master's degree and deposited in the University of Kentucky Library are as a rule open for inspection, but are to be used only with due regard to the rights of the authors. Bibliographical references may be noted, but quotations or summaries of parts may be published only with the permission of the author, and with the usual scholarly acknowledgments.

Extensive copying or publication of the thesis in whole or in part also requires the consent of the Dean of the Graduate School of the University of Kentucky.

A library that borrows this thesis for use by its patrons is expected to secure the signature of each user.

Name	Date

THESIS

Yali Liang

The Graduate School

University of Kentucky

2010

DRUG RELEASE AND PHARMACOKINETIC PROPERTIES OF LIPOSOMAL DB-67

THESIS

A thesis submitted in partial fulfillment of the
requirements for the degree of Master of Science in the
College of Business and Economics
at the University of Kentucky

By

Yali Liang

Lexington, Kentucky

Director: Dr. Markos Leggas, Professor of Pharmaceutical Science

Lexington, Kentucky

2010

ACKNOWLEDGEMENTS

The following thesis benefited from the insights and direction of several people. First, I would like to thank my major advisor, Dr. Markos Leggas for providing this wonderful opportunity for me to grow as a scientist. I had learned critical thinking and reasoning through working with him, which I believe will be very beneficial for my future profession. I will always be grateful for the education, guidance and mentorship he has provided. I would like to thank Dr. Brad Anderson for his continuous support and valuable advice through the course of this work. I am grateful for his patience to answer many of my questions and his expertise to guide the direction of the research. I also acknowledge the contributions of my committee member Dr. Patrick McNamara, whose suggestions guided and challenged my thinking.

I really appreciate the assistance of Dr. Jamie Horn with HPLC assays, Dr. Paul Bummer with osmolality detection, Eyob D. Adane with animal experiment and Melissa Howard with light scattering particle sizer. I would also like to thank the members of the Leggas Lab, past and present, Dr. Mamta Goswami, Dr. Dominique Talbert, Eleftheria Tsakalozou, Kuei-Ling Kuo, Tamer A. Ahmed, and Marta Mazik for their support and caring, and the members of Anderson Lab, Dhaval Patel, Kyle Fugit, and especially Dr. Tian-Xiang Xiang and Sweta Modi, for so many thoughtful discussions.

In addition to the scientific and technical assistance above, I received equally important assistance from the family. I would like to thank my husband, Zhiwei Liu, for his continuous love and support throughout my graduate study. I also wish to thank all my family members for their love and encouragements.

TABLE OF CONTENTS

LIST OF TABLES

LIST OF FIGURES

Chapter One Statement of Aims

The objective of this thesis is to characterize the drug release and the pharmacokinetic properties of a liposomal formulation of the camptothecin analogue DB-67. It has been shown that DB-67 has potent anti-tumor activity *in vitro* and *in vivo* [Bence et al. 2004; Bom et al. 2000; Bom et al. 2001; Burke and Bom 2000; Lopez-Barcons et al. 2004; Pollack et al. 1999]. It is superior to other camptothecins in that it demonstrates relatively higher lactone stability than other analogues in plasma due to the decreased association of carboxylate with human serum albumin (HSA) and the increased lipid membrane partitioning. However, because of the rapid elimination of DB-67 (elimination half-life 1.4 hr for human)[Arnold et al. 2010], it requires frequent administration to maintain efficacious drug concentrations within the plasma. In vitro studies have demonstrated that liposomal formulations have the advantage of extending the elimination half-life of the active agent, minimizing the toxicities and enhancing efficacy. For example, liposomal formulations of doxorubicin and daunorubicin have prolonged plasma half-lives and improved tumor site specific accumulation as compared to non-liposomal formulations [Boiardi et al. 1999; Forssen et al. 1996; Hussein 2003; Muggia 1997; Vorobiof et al. 2003; Ying et al. 2009]. Unfortunately, previous attempts to develop liposomal formulations of DB-67 were not successful because they did not demonstrate improved pharmacokinetics [Zamboni et al. 2008]. The goal of this thesis is to characterize the drug release and pharmacokinetics of a sterically stabilized liposomal formulation of DB-67 and to investigate the factors influencing the drug release and pharmacokinetics. The following specific aims were explored as part of this work.

a) Characterize cholesterol content, particle size, and drug-to-lipid ratio effects on DB-67 release rate from liposomes *in vitro* with a dynamic dialysis model.
b) Determine cholesterol content and particle size effects on the pharmacokinetics of liposomal DB-67 *in vivo*.
c) Investigate the lipid dose effect on the pharmacokinetics of liposomal DB-67 and determine the proper lipid dose to be used in the future development.
d) Evaluate the effects of cholesterol content, particle size and lipid dose on the reticuloendothelium system (RES) uptake of DB-67 loaded liposomes *in vivo*.

Chapter Two Introduction

I. Liposomes as Drug Delivery Systems

Liposomes are one of the most tested and versatile systems among all the lipid-based nanotechnologies for drug delivery. They are composed of lipid bilayers enclosing an aqueous core in the center (see Figure 2.1). Drugs can be either loaded into the aqueous core or bound to the lipids within the membrane. In either case, the lipid bilayer serves as a barrier preventing drugs from being released. The sizes of liposomes range from 1 μm for multilamellar vesicles (MLV) to 4-8 nm for very small particles[Mayer et al. 1989]. Since the liposomes in clinical use have an average size of 50 to 200 nm, liposomes are commonly referred to as nanoparticles.

Based on their composition, liposomes are generally classified as either conventional or sterically stabilized liposomes, also known as "stealth" liposomes (See Figure 2.1). Conventional liposomes are composed of simple lipid bilayers typically possessing high phosphatidylcholine (PC) and cholesterol (Chol) content. Sterically stabilized liposomes or "stealth" liposomes are lipid bilayers coated with either a ganglioside GM1 or synthetic neutral polymer polyethylene glycol (PEG) [Allen et al. 2006; Allen and Chonn 1987]. This coating stabilizes the liposomes by reducing the binding of serum opsonins, as well as by minimizing their interaction with the reticuloendothelium system (RES) [Allen and Hansen 1991; Huang et al. 1992; Lasic et al. 1991]. Therefore, the "stealth" liposomes stay in the circulation for an extended period of time.

Liposomes have been successfully used in the delivery of anti-cancer agents, and liposomal formulations of doxorubicin (Myocet, Doxil) and daunorubicin (DaunoXome) have been approved by the Food and Drug Administration (FDA) for clinical use. Developing liposomal formulations for anti-cancer agents holds great interest in research because they have certain advantages. Firstly, liposomes may serve as a sustained drug release system [Drummond et al. 2008], which results in prolonged elimination half-life of the active agent. Anti-tumor drugs are cell-cycle dependent and they require continuous administration to exert the maximum anti-tumor effect [Burris et al. 1992; Georgiadis et al. 1997; Gomi et al. 1992; Johnston et al. 2006]. The extended elimination half-life provided by liposomal formulation may lead to a decrease in the frequency and length of drug administration [Kim et al. 2001; Kirpotin et al. 2006]. Secondly, liposomes increase site-specific accumulation of anti-cancer agents at tumor tissues [Drummond et al. 2008]. Most normal tissues have fenestrated vasculature [Lum and Malik 1994], but the accumulation of drug loaded liposomes in these tissues is minimal because the pore size is smaller than most liposomes. In contrast, the fast growing nature of tumors results in disorganized vascular endothelium

with larger fenestrations, which leads to the increased extravasation of liposomes at the tumor sites. This effect is often referred to as the enhanced permeability and retention (EPR) effect [Matsumura and Maeda 1986]. Usually, significantly reduced volume of distribution and improved therapeutic index are achieved in liposomal delivery systems [Messerer et al. 2004; Waterhouse et al. 2001]. All the above advantages rely on the extended elimination half-life of the liposomal drug. To obtain it, we need to understand the elimination process of the liposomal drug, which not only depends on the drug itself, but also depends on the clearance of the liposomal carrier from the circulation, and the release rate of the entrapped drug from the liposomal carrier [Drummond et al. 2008]. In the development of a new liposomal formulation, the last two processes have to be taken into account in order to achieve the maximum benefit. The following sections will discuss the factors that influence these two rates.

II. Factors Influencing Liposomal Pharmacokinetics

The physicochemical properties of the liposomal carrier, lipid dose, dosing schedule, route of administration, and the drug that is encapsulated affect the pharmacokinetics of the liposomal carrier [Drummond et al. 1999]. In the context of this work, we focus on cholesterol content, particle size, and lipid dose given that they can influence loading and release of the lipophilic DB-67 from liposomes.

Inclusion of cholesterol in the liposomal composition leads to a decrease in liposomal clearance and an increase in liposomal elimination half-life. An inverse relationship was observed between the percentage of incorporated cholesterol and the liposome plasma clearance [Semple et al. 1996]. In most cases, over 33% (molar ratio) of cholesterol is used to maintain sufficiently long half-lives of liposomes in the blood.

Increasing of liposomal particle size results in an increase of liposomal clearance from the circulation [Klibanov et al. 1991; Litzinger et al. 1994]. When the diameter of the liposomal particle is larger than 200 nm, the blood clearance is dramatically increased and about 81% of injected lipid dose is taken up into the RES at 5 hr after intravenous injection [Klibanov et al. 1991]. It is widely accepted that liposomes with the diameter of 100 to 200 nm have the greatest level of tumor accumulation [Charrois and Allen 2003; Ishida et al. 1999; Mayer et al. 1989; Nagayasu et al. 1999].

The effect of lipid dose on the pharmacokinetics of liposomes is dependent on lipid composition in that conventional liposomes typically display saturable nonlinear pharmacokinetics, whereas sterically stabilized liposomes demonstrate linear pharmacokinetics over a wide range of doses [Allen et al. 2006; Allen and Hansen 1991]. For instance, in liposomes composed of egg phosphatidylcholine and cholesterol (PC:Chol 2:1), the lipid elimination half-life increased from 6.9 to 13.0 hr as the lipid dose was increased from 2.0 to 10.0 μmol/mouse [Allen and Hansen 1991]. It is worth noting that all the above observations are from blank liposomes. The pharmacokinetics of liposomes may be altered when the active drug is encapsulated. For a specific liposome system, one has to examine the effect of each factor on the pharmacokinetics of drug associated liposomes to optimize it for clinical development.

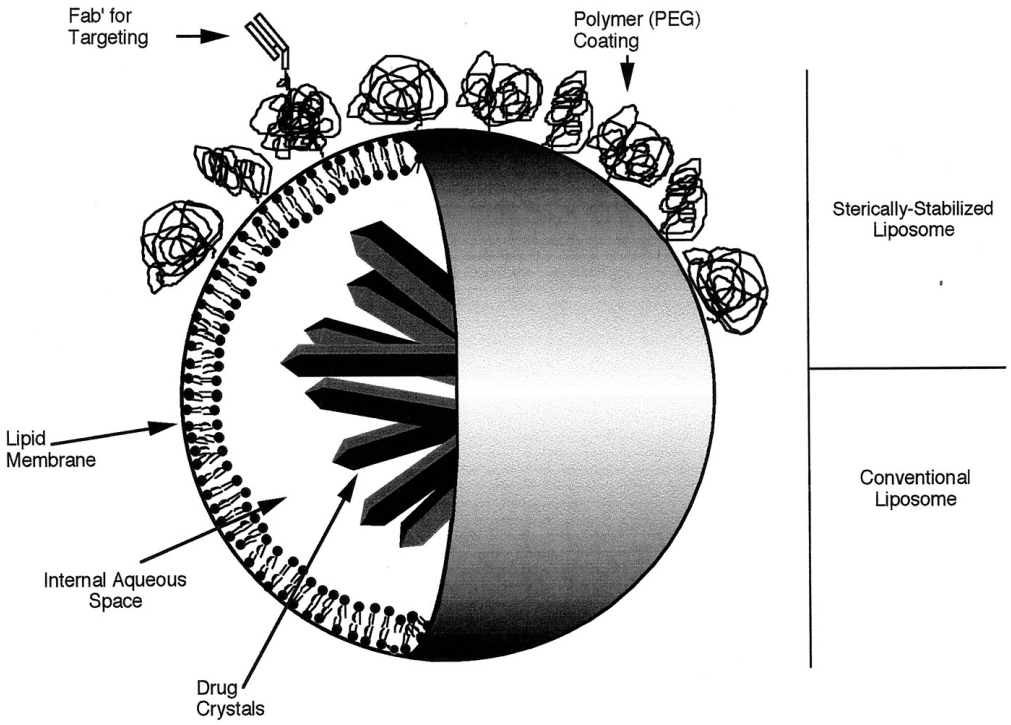

Figure 2. 1 Structure of conventional and sterically-stabilized liposome [Drummond et al. 1999].

III. Factors Influencing Drug Release Rate from Liposomes

The most important factors influencing drug release rate from liposomes are the drug loading method, as well as the physicochemical properties of the lipid membrane and the entrapped therapeutic agent. In the scope of this thesis we are interested in cholesterol content and drug-to-lipid ratio.

The effect of cholesterol content on drug release from liposomes demonstrates a drug-dependent manner. Cholesterol incorporation led to an increases of the retention of ara-C [Mayhew et al. 1979] and doxorubicin [Mayer et al. 1985]. However, in a study by Dos Santos et al., inclusion of cholesterol (45 mole %) dramatically increased the release of idarubicin from liposomes, as demonstrated by a 15-fold higher idarubicin concentration remained in the plasma at 2 hr post dosing when cholesterol free liposomes were administered as compared to cholesterol containing liposomes [Dos Santos et al. 2002].

Interestingly, the effect of drug-to-lipid ratio on drug release is also dependent on the specific drug entrapped. In the case of doxorubicin, higher drug-to-lipid ratio resulted in decreased drug retention half-life [Mayer et al. 1990]. In contrast, vincristine and irinotecan were retained longer in liposomes with higher drug-to-lipid ratio [Johnston et al. 2006], corresponding to increases in release half-life of more than 10-fold as drug-to-lipid ratio was increased from 0.05 to 0.6 (w:w). The complexities of these effects further emphasize the necessity of using drug loaded liposomes, not only the blank ones, to investigate the effects of factors influencing pharmacokinetics of the formulation.

IV. Camptothecin and its Application in Chemotherapy

Camptothecin was first isolated from the bark of the Chinese tree, *Camptotheca acuminate* [Pommier 2006]. Despite potent anti-tumor efficacy *in vitro*, the clinical development of camptothecin was halted due to toxicities including diarrhea, neutropenia, thrombocytopenia, hemorrhagic cystitis and leukopenia [Muggia and Burris 1994]. Biochemical studies demonstrated that camptothecin exerts its pharmacological effect via interaction with the nuclear enzyme, Topoisomerase I (Topo I) [Eng et al. 1988; Hsiang et al. 1985]. During cell replication and transcription, Topo I relaxes supercoiled DNA. In this process, Topo I binds to double stranded supercoiled DNA, nicking one of the strands, which enables the rotation of the intact DNA strand around the break and facilitates DNA relaxation [Eng et al. 1988]. Subsequently, Topo I religates the nicked DNA and moves to the next coiled DNA segment. Thus, under normal conditions, the single

strand DNA break is transient. However, when camptothecin or its analogues are present, the drug interacts with the Topo I/DNA complex and inhibits the religation step. Ultimately, some single stand DNA breaks are converted to double strand breaks when additional enzymes and proteins, comprising the replication machinery, collide with the Topo I/DNA/camptothecin complex. These double strand breaks can lead the cell into apoptosis and cell death [Eng et al. 1988]. This mode of action indicates that camptothecins are primarily S-phase specific drugs and that their cytotoxic effect depends on active DNA replication or transcription. Generally, tumor tissues have more cells undergoing replication, so they are more susceptible to camptothecin than most normal tissues.

Camptothecin undergoes a reversible hydrolysis of the α-hydroxy-δ-lactone ring to form camptothecin carboxylate and the process is pH-dependant (Figure2.2 A). Early *in vitro* studies demonstrated that the pharmacologic activity of camptothecin was greater when the drug was in the lactone form. *In vivo*, the stability of lactone was further compromised by the affinity of the carboxylate moiety for plasma albumin. In contrast to this, the toxicity experienced by patients receiving the sodium carboxylate demonstrated that the *in vivo* activity may be due to the conversion of the carboxylate back to the lactone form, which is likely a tissue dependent dynamic process. Thus, the unpredictable stability of camptothecin molecule, coupled with the prevalent toxicities led researchers to develop analogues with greater lactone stability and potentially more predictable efficacy and toxicities.

Currently only two camptothecin derivatives, topotecan (Hycamtin®) and irinotecan (also known as CPT-11, Camptosar®), have been approved by the FDA for clinical use (Figure 2.2 B). Topotecan was approved first to treat ovarian cancer in 1996, then later for treatment of cervical cancer and small cell lung cancer. It has significantly higher solubility in the lactone form than camptothecin because of the ethyldimethylamino substitution on the B-ring [Dancey and Eisenhauer 1996; Pommier 2006]. In addition, structural studies investigating the interaction of topotecan with Topo I have demonstrated that its carboxylate form is also present in the Topo I/DNA/topotecan complex suggesting that the inactivity of camptothecin carboxylate shown in biochemical studies may not necessarily apply to its analogues. In 1996, irinotecan was approved to treat metastasized colorectal cancer or recurring colorectal cancer [Pommier et al. 1998]. It is a prodrug and is activated by carboxylesterases to SN-38 in plasma and tissues. This active metabolite is 1000-fold more potent than the parent compound, irinotecan [Garcia-Carbonero and Supko 2002].

Burke and Bom synthesized a dual 7, 10 – modified camptothecin, 7-t-butyldimethylsilyl-10-hydroxy camptothecin (DB-67), which showed increased human blood stability and potent anti-tumor activity (Figure 2.2 C) [Bom et al. 1999; Bom et al. 2000; Bom et al. 2001]. *In vitro* studies investigating the hydrolysis of DB-67 in plasma showed that over 30% of lactone form remains at equilibrium. This is significantly higher than topotecan (~12%) and irinotecan (~21%) [Bom et al. 2001] and has been attributed to the 7 position alkylsilyl group substitution. This structural modification renders DB-67 25- to 50-fold more lipophilic than camptothecin, 100 times more lipophilic than topotecan and about 15 times more lipophilic than SN-38 [Bom et al. 2001]. The high lipophilicity facilitates lactone partitioning into red blood cells, which also prevents hydrolysis. In addition, the 7 and 10 position dual-substitution reduces the binding of DB-67 carboxylate to HSA, so that more lactone is retained in the plasma [Burke and Bom 2000].

In vitro cytotoxicity assays, using cell lines from eight distinct tumor types, showed that DB-67 had comparable potency as irinotecan and topotecan [Bom et al. 2001]. Preclinical studies in mice demonstrated that DB-67 was very potent in tumor inhibition [Burke and Bom 2000; Lopez-Barcons et al. 2004; Pollack et al. 1999]. When DB-67 was administrated as lactone or carboxylate form, approximately 80% or 50% of the drug was in the lactone form at 1 hr post injection, respectively [Adane et al. 2010]. When mouse subcutaneous xenograft models (U87 malignant glioma cell line) were treated with 3 or 10 mg/kg/day DB-67 subcutaneously for 5 consecutive days in a 21-day cycle, the treatment groups had a significant delay in tumor growth as compared to control group at 28 days after implantation [Pollack et al. 1999]. Collectively the *in vivo* stability and efficacy studies demonstrated that this agent warranted clinical testing.

Currently, DB-67 is undergoing Phase I and II clinical trials for the treatment of refractory or metastatic solid malignancies and myelodysplastic syndrome. The first in human phase I study of DB-67 showed that this agent was well tolerated and patients receiving a daily intravenous dose for five consecutive days experienced dose dependent hematologic toxicities that were typically resolved within a 21-day dosing cycle. Interestingly, these patients did not experience diarrhea, which is typical with other camptothecin analogues [Arnold et al. 2010]. Although the current intravenous formulation of DB-67 allows its further clinical development, the need to administer camptothecins in a protracted dosing schedule points to the need for an alternative formulation that may augment efficacy by increasing drug localization in the tumor while minimizing systemic toxicities.

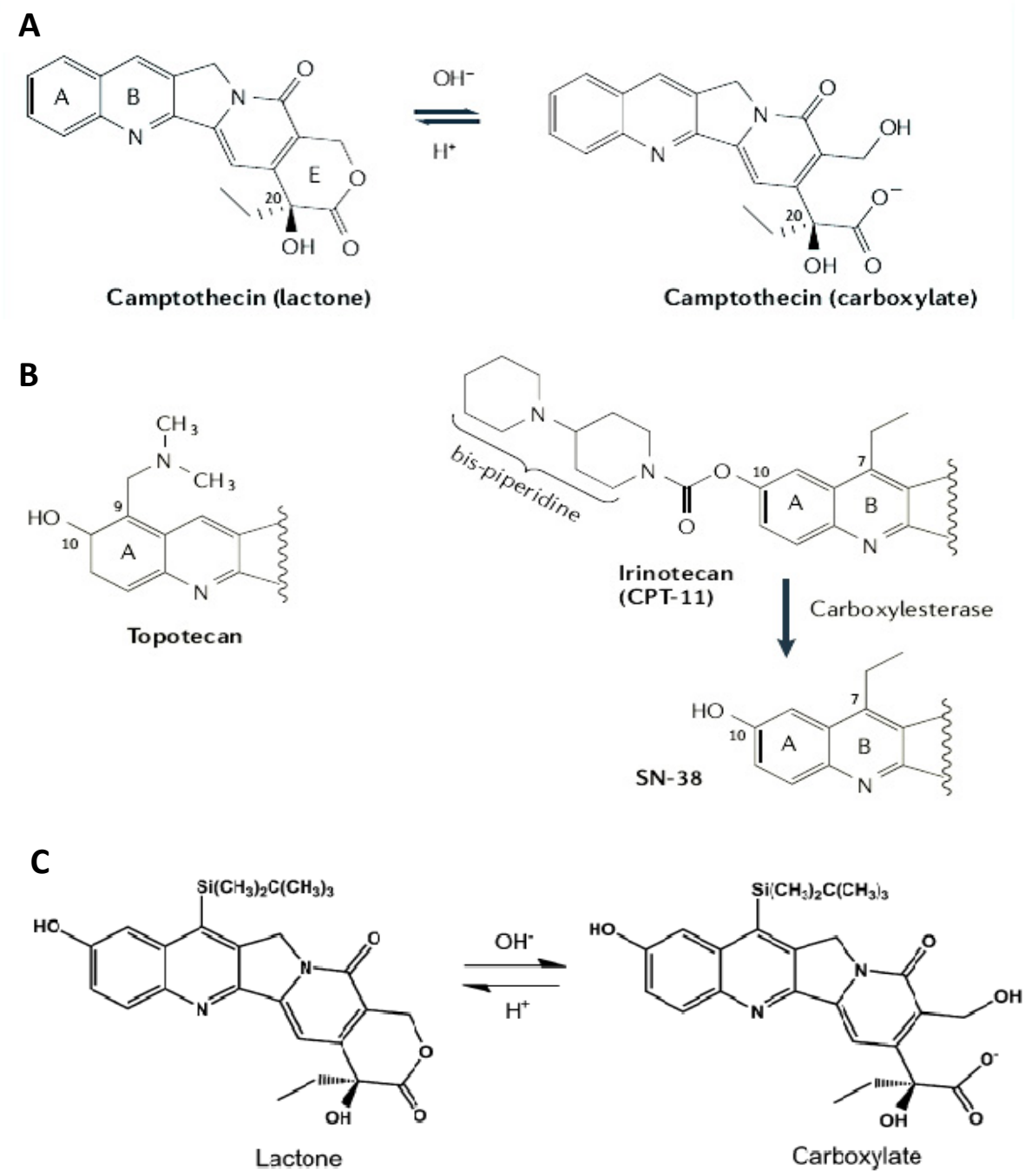

Figure 2. 2 The chemical structures of camptothecin and its derivatives.
(A) Chemical structures of camptothecin lactone and carboxylate. The two forms interconvert in a pH-dependent manner [Pommier 2006]. (B) The two FDA approved camptothecin derivatives, topotecan and irinotecan. Irinotecan has to be hydrolyzed to yield its active metabolite SN-38 [Pommier 2006]. (C) Chemical structures of DB-67 lactone and carboxylate. The two forms interconvert in a pH-dependent manner [Adane et al. 2010].

V. Development of Liposomal DB-67 Formulation

We proposed to apply liposomal formulation for DB-67 delivery because: 1) liposomal formulation prolongs the circulation lifetime of the active drug [Allen et al. 1995] thus decreasing the required frequency or length of drug administration, 2) liposomal formulation acts as a sustained release system, which mimics the protracted dosing regimen for cancer treatment and leads to the enhanced anti-tumor efficacy [Drummond et al. 2008]. An in *vivo* efficacy study demonstrated that the protracted dosing of DB-67 yielded significantly improved survival fraction in a mouse subcutaneous xenograft model using H460 non-small cell lung cancer cell line (Adane and Leggas, unpublished data). Tumor bearing mice were treated with the DB-67 maximum tolerance dose (MTD, 7.5 mg/kg daily intravenous dose for five consecutive days in a twenty-one day cycle) or protracted dose (either 3.75 mg/kg daily intravenous dose for ten consecutive days or 2.5 mg/kg daily intravenous dose for fifteen consecutive days in a 21-day cycle). After one cycle of treatment, two out of ten mice survived in MTD group in comparison with six or eight out of ten mice survived in the protracted dosing groups. However, the administration of multiple doses to cancer patients is not ideal as the disease compromises their overall health. Therefore, the ultimate goal of this work is to utilize liposomes in the DB-67 delivery to render the potent anticancer agent more efficacious in the tumor sites and less toxic in the normal tissues.

So far, liposome formulations for DB-67 delivery have been investigated in conventional liposomes and sterically stabilized liposomes, however, neither one of them achieved extended elimination half-life of DB-67 [Lopez-Barcons et al. 2004; Zamboni et al. 2008]. 1,2-dimyristoyl-sn-glycerol-3-phosoho-sn-1-glyercol (DMPC) and 1,2-dimyristoyl-sn-glycerol-3-phospho-sn-1-glyercol (DMPG) (DMPC:DMPG 7:3, mol/mol) were applied as the major components of these liposomes. Upon its injection into mice, DB-67 was immediately released from the liposomes and the liposomes only acted as an intravenous vehicle, instead of a drug carrier [Lopez-Barcons et al. 2004; Zamboni et al. 2008]. Joguparthi and Anderson proposed to use "stealth" liposomes (stabilized with PEG) with highly saturated lipid (1, 2-distearoyl-sn-glycero-3-phosphatidylcholine, DSPC) as the major component (DSPC:m-PEG-DSPE 95:5 mole %) to develop liposomal formulation of DB-67 [Joguparthi and Anderson 2008]. In the study, DB-67 was loaded into liposomes as carboxylate (pH 9.5) and the formulation showed a prolonged drug retention half-life of 13.5±2.7 hr in plasma [Joguparthi and Anderson 2008]. Despite the promising retention half-life *in vitro*, pharmacokinetic studies with this formulation showed that the clearance of the vesicles was rapid and the release of DB-67 from the liposomes was estimated to be more rapid [Joguparthi et al. 2008a]. The purpose of this thesis is to investigate the factors influencing drug release

and pharmacokinetics of the sterically stabilized liposomal formulation of DB-67. Ultimately, improved anti-cancer efficacy and minimized toxicities are anticipated by controlling the factors appropriately.

In the following studies, we first explored the effect of cholesterol content, particle size and drug-to-lipid ratio on DB-67 release *in vitro*. Subsequently, by using a 2 × 2 factorial experimental design, we determined the effect of cholesterol content (40 vs. 0 mole %) and particle size (~180 vs. ~120 nm) on the pharmacokinetics of liposomal DB-67 *in vivo*. Then, we investigated the effect of lipid dose on the pharmacokinetics of liposomal DB-67. Finally, the RES uptake of DB-67 loaded liposomes was determined and the mechanisms driving the effect of each factor were also discussed.

Chapter Three Materials and Methods

I. Materials

DB-67 was provided by Novartis Pharmaceuticals Corporation (East Hanover, NJ). Dialysis tubes (Float-A-Lyzer, MWCO:100KD) were obtained from Spectrum Laboratories (Rancho Dominguez, CA). Phospholipids 1, 2-distearoyl-sn-glycero-3-phosphatidylcholine (DSPC, >99% purity) and 1, 2-distearoyl-sn-glycero-3-phosphoethanolamine-N-[methoxy-polyethylene glycol 2000] (m-PEG DSPE, MW = 2806, >99% purity) were purchased from Avanti Polar Lipids (Alabaster, AL). Polycarbonate membranes (pore size of 0.1 μm or 0.2 μm, thickness of 25 mm) were purchased from GE water & Process Technologies (Trevose, PA). Heparin (heparin sodium 1000 IU) was obtained from Baxter (Deer Field, IL). Cholesteryl hexadecyl ether ([Cholesteryl-1,2-^{3}H(N)]-, >97%, 250 μCi (9.25 MBq), [^{3}H]-CHE) was purchased from PerkinElmer (Waltham, MA). AquaSil™ siliconizing reagent was obtained from Pierce (Rockford, IL). TS-2 ™ tissue solubilizer was obtained from Research Products International Corp. (Mount Prospect, IL). All the other reagents were purchased from Fisher Scientific (Fair Lawn, NJ).

II. Preparation of Liposomes

Two types of lipid composition were used in the present study, cholesterol free (DSPC:m-PEG DSPE 95:5 mole %) and cholesterol containing (DSPC:m-PEG DSPE:cholesterol 55:5:40 mole %). Certain amount of the lipids, DSPC, m-PEG DSPE, and cholesterol were weighed and dissolved in chloroform, and then distributed in test tubes. The stock total lipid concentration was 60 mg/ml for the *in vitro* experiments, 20 mg/ml or 60 mg/kg for the *in vivo* studies depending on the lipid doses used (60 mg/kg for lipid dose of 704 mg/kg, and 20 mg/kg for the lipid doses of 64 mg/kg or ~250 mg/kg). To determine the lipid concentration, trace amount of [^{3}H]-CHE was added to the lipid solution (20 μl of [^{3}H]-CHE (20 μCi) was added to 6 ml of the lipid chloroform solution). The organic solvent was evaporated under a stream of nitrogen and a thin film of lipid was formed inside of the test tubes. The tubes were vacuum-dried overnight at 40°C to remove any residual organic solvent. The dried lipid film was hydrated with DB-67 solution (pH 9.5, 298 mOsm) at 60°C in a water bath with vigorous shaking to obtain a lipid suspension. The DB-67 solution was prepared by dissolving DB-67 powder in 85 mM sodium carbonate buffer (pH 11) followed by stirring for 2 to 3 hr until a clear solution was obtained. The pH of the solution was adjusted to 9.5 with hydrochloric acid (HCl, 1M). DB-67 concentration of the solution was 2 mM and 20 mM for the drug-to-lipid ratios of 0.03 and 0.3 (w:w), respectively, in the *in vitro* experiments. DB-67 concentration was 0.67 mM and 2 mM for the lipid concentration of 20 and 60 mg/ml, respectively, to keep the drug-to-lipid ratio constant (0.03 w:w) in the *in vivo* studies. The lipid suspension was extruded through two stacked polycarbonate membranes (pore size of 100

nm or 200 nm) ten times with an extrusion device (Liposofast®, Avestin, Ontario, Canada) at 60°C. Following preparation, liposomes were cooled to room temperature for 3 hr. Then they were stored at 4°C until the experiments were conducted. Formulations used for pharmacokinetic studies were prepared the day before the experiment and dialyzed against 2 L of 85 mM sodium carbonate buffer at 37°C (pH 9.5, 298 mOsm) for 12 hr to remove free DB-67. Dialyzed liposomes were used within 24 -28 hr.

III. Characterization of Liposomes

Liposomal particle size was determined by dynamic light scattering (DSL, Delsa™ Nano C Particle Analyzer, Beckman Coulter, Center Valley, PA). Liposomes prepared from polycarbonate membrane with pore size of 100 nm ranged from 103 to 121 nm and liposomes prepared from 200 nm polycarbonate membrane ranged from 167 to 187 nm in diameter. Osmolality was determined by the freezing point detection using a Fiske One-Ten Osmometer (Fiske Associates, Norwood, MA).

IV. *In vitro* Drug Release Experiment

Drug release rates from liposomes were determined through a dynamic dialysis procedure described previously [Joguparthi et al. 2008b]. Briefly, after liposomes were prepared by the hydration-extrusion method described above, DB-67 loaded liposome suspension was transferred into a dialysis tube. The dialysis tube (Float-A-Lyzer, MWCO:100KD, 5 ml, Spectrum Laboratories, Rancho Dominguez, CA) was preconditioned in deionized water for 15 min and then in dialysis buffer (described below) for 30 min. Subsequently, the liposomes containing dialysis tube was dialyzed against 2 L of 85 mM sodium carbonate buffer at 37°C (pH 9.5, 298 mOsm) for 12 hr to remove free DB-67. Following dialysis, the liposome suspension was transferred to another preconditioned dialysis tube and dialyzed against 2 L of carbonated phosphate buffered saline (C-PBS, pH 7.4, 298 mOsm) at 37°C for 24 hr. C-PBS buffer was prepared by adding 24 mM sodium carbonate buffer to phosphate buffered saline (PBS). At 1, 2, 3, 5, 9, 13 and 24 hr, 20 µl of sample was taken from inside of the dialysis tube and diluted into 980 µl cold (-20°C) methanol:acetonitrile (2:1, v/v) and stored at -20°C until HPLC analysis.

V. Pharmacokinetic Experiments

Cholesterol free and cholesterol containing formulations of liposomal DB-67 were prepared and dialyzed with the method described above. Non-liposomal DB-67 formulation was DB-67 lactone with β-cyclodextrin sulfobutyl ether (SBE-CD, Captisol®) as excipient. All animal experiments were approved by the University of Kentucky Institutional Animal Care and Use Committee. Female C57/BL6 mice weighing from 23-31 g (Harlan, Indianapolis, IN) were used in the *in vivo* experiments. All mice were obtained at least 2 weeks prior to use and maintained within a con-

trolled temperature (22±1°C) and humidity (60±10%) environment. We used sparse sampling in the pharmacokinetic experiment. A total of 9 mice were used in each experiment, and they were randomly selected into 3 small groups with 3 mice within each group. Liposomal DB-67 was administered intravenously in the lateral tail vain and blood (90 µl) was collected through the saphenous vein in a hematocrit capillary tube (Fisher Scientific, Fair Lawn, NJ) at 0.087, 0.5, 1, 1.5, 3, 6, 12, 24 and 36 hr (the detailed dosing and sampling time information is shown below in Table 3.1. The targeted lipid dose in the factorial experiment (investigating the cholesterol and particle size effects on lipid clearance) was 250 mg/kg, and the targeted low and high lipid doses in the dose escalation study were 60 and 700 mg/kg, respectively (see Table 4.5 for the specific doses used in each experiment). The injection volume was proportional with body weight (grams of body weight ×10 µl per mouse). After collection, the blood was explelled into a pre-heparinized and siliconized 1.5-ml micro-centrifuge tube, then kept on ice. The whole blood was centrifuged at 8,500 g for 3 min to separate the plasma. An aliquot of the plasma (20 µl) was transferred into a scintillation vial for counting in order to determine the lipid content. Another aliquot of plasma (30 µl) was transferred to a 1.5 ml amber siliconized micro-centrifuge tube (Crystalgen Inc., Plainview, NY) which contained 120 µl of cold methanol (-80°C). After shaking vigorously for 10 sec, it was again centrifuged at 8,500 g for 3 min. The supernatant was transferred into another 1.5 ml amber siliconized micro-centrifuge tube to be stored at -80°C until HPLC analysis. At 12, 24, and 36 hr after the injection of liposomal DB-67, the mice were anesthetized and then bled by cardiac puncture. Livers and spleens were collected, blot dried, weighed, and wrapped in aluminum foil prior to being snap frozen in liquid nitrogen. The tissues were stored in -20°C until scintillation counting to determine the lipid content. Non-liposomal DB-67 (1.0 mg/kg) was administered to a group of mice intravenously. Blood (50 µl) was collected and processed as indicated above at 0.087, 0.5, 0.75, 1.5, 3 and 6 hr post injection.

Table 3. 1 The dosing and sampling time of mice in pharmacokinetic experiment*.

Group #	Sampling Time			Injection Day
Group 1	1 h	3 h	36 h	Day 1
Group 2	30 min	6 h	24 h	Day 1
Group 3	5 mim	1.5 h	12 h	Day 2

*Sparse sampling was used in the pharmacokinetic experiment. A total of 9 mice were randomly selected into 3 small groups with 3 mice within each group. Liposomal DB-67 was administered intravenously in the lateral tail vain and blood was collected through the saphenous vein at 0.087, 0.5, 1, 1.5, 3, 6, 12, 24 and 36 hr post injection. The experiment was completed in two consecutive days with group 1 and 2 injected on Day 1 and group 3 injected on Day 2**.**

VI. HPLC Analysis

DB-67 lactone and carboxylate plasma concentrations were quantified by an HPLC method as described previously [Horn et al. 2006]. A Shimadzu HPLC system (Shimadzu Inc., Atlanta, GA) controlled by Class-VP integrating software (Version 7.4) was used for the analysis. The system consisted of an in-line degasser (DGU-14A), a LC-10AD VP pump, a refrigerated autoinjector (Shimadzu SIL-10AD VP) with rack temperature at 4°C, and a fluorescence detector (RF-10XL) set at 380 nm (excitation wavelength) and 560 nm (emission wavelength). A reversed-phase C18 analytical column (Waters Nova-Pak C18 4μm; 3.9 x 150 mm) fitted with a guard column (Waters Nova-Pak C18 4μm; 3.9 x 20 mm) was used to separate analytes. The retention time was 3.2 min for DB-67 carboxylate and 9.8 min for lactone. The mobile phase consisted of 0.15 M ammonium acetate (NH_4OAc) containing 10 mM tetrabutylammonium dihydrogenphosphate (TBAP, pH 6.5) and acetonitrile (65:35, v/v). The flow rate was 1 ml/min and the total run time was 12 min. The extracted plasma samples were diluted with an equivalent volume (40 μl) of mobile phase buffer prior to injection and samples were injected within 6 hr of preparation to prevent the inter-conversion between lactone and carboxylate. Calibration curves were linear in the range of 2.5-100 ng/ml for carboxylate and 5-300 ng/ml for lactone.

Samples from *in vitro* drug release experiments were analyzed with the same HPLC system. DB-67 carboxylate and lactone standards were prepared in an ice cold mixture of organic solvent (methanol:acetonitrile 2:1; v/v) with the lipid (DSPC) concentration of 60 μg/ml. Linear calibration curves ranged 10 – 5000 ng/ml for both carboxylate and lactone (with the detector at low sensitivity setting). In all cases, the samples were diluted with an equivalent volume (40 μl) of mobile phase buffer prior to a 50 μl injection. Injections were within 6 hr of preparation.

VII. Lipid Content Analysis in Plasma and Tissues

a. Sample preparation

To analyze the lipid concentration in plasma, 20 μl of plasma was transferred into a scintillation vial, and subsequently acidified with 40 μl of glacial acetic acid (Fisher Scientific, Pittsburgh, PA). Ten ml of Bio-Safe II™ scintillation cocktail (Research Products International Corp., Mount Prospect, IL) was added to each sample and kept in dark at room temperature for 15 min before scintillation counting. To analyze the lipid amount in tissues, about 100 mg of liver or the whole spleen were weighed and placed into a 25 ml scintillation vial. Tissues were solubilized with 1 ml of TS-2 ^{TM} tissue solubilizer (Research Products International Corp., Mount Prospect, IL) and digested at 50°C until the tissues were completely dissolved. Then, the tissue samples were decolo-

rized with 200 µl of 30% H_2O_2 (Fisher Scientific, Fair Lawn, NJ), and 40 µl of glacial acetic acid were added to eliminate chemiluminescence. Ten ml of Bio-Safe II™ scintillation cocktail was added to each sample and kept in dark at room temperature for 15 min before scintillation counting.

b. Scintillation counting

Radioactivity of each sample was measured with a scintillation counter (CARB® 2200CA, Packard Instrument Co., Downer Grove, IL). The lipid concentrations in plasma and tissues were calculated based on the radioactivity as described below.

c. Methods for estimating lipid concentration

The radioactivity measured by scintillation counting was given in DPM, and the lipid concentration and the percentage of injected lipid dose was calculated based on equations shown below.

1. Radioactivity in the plasma or tissues was converted from DPM to µCi based on Equation 1.

$$1\mu Ci = 2.22\times10^6 \text{ DPM} \quad \text{(Eq.1)}$$

2. Lipid concentration in the plasma was calculated based on Equation 2.

$$LipidConc(mg/ml) = \frac{R\times 6}{20}\times 1000 \quad \text{(Eq.2)}$$

Where, LipidConc represents the lipid concentration in plasma as mg/ml. R represents the measured radioactivity of plasma sample in µCi, and 20 is the volume (µl) of plasma used for scintillation counting. The lipid (mg) to radioactivity (µCi) ratio is 6. For the experiments of high lipid dose (704 mg/kg), the ratio is 18.

3. Lipid amount in the tissues was calculated based on Equation 3.

$$LipidAmount(mg) = \frac{R\times 6\times W2}{W1} \quad \text{(Eq.3)}$$

LipidAmount is the lipid amount in the whole tissue (liver or spleen) in mg. R represents the measured radioactivity of tissues as µCi and the lipid (mg) to radioactivity (µCi) ratio is 6. For the experiments of high lipid dose (704 mg/kg), the ratio is 18. W1 represents the weight of the tissue used for scintillation counting in grams, and W2 is the weight of the whole tissue in grams.

4. Percentage of injected lipid dose remained in the blood was determined based on Equation 4.

$$\%injectedDose = \frac{LipidConc_{blood} \times B.W. \times 6\% / 1.06}{lipidDose \times B.W. / 1000} \times 100 \quad \text{(Eq.4)}$$

%injectedDose represents the percentage of injected lipid dose remaining in the blood. $LipidConc_{blood}$ is the lipid concentration in the whole blood in mg/ml, which is derived from lipid concentration in the plasma assuming the hematocrit is 45% [Drummond et al. 2009]. B.W. is the body weight of the mouse in grams. Blood weight is assumed to be 6% of the body weight [Drummond et al. 2009] and the blood density is 1.06 g/ml [Cutnell and Johnson 1998]. LipidDose represents the lipid dose for I.V. injection in mg/kg.

5. Percentage of injected lipid dose taken up into the tissues was determined based on Equation 5.

$$\%injectedDose = \frac{LipidAmount}{lipidDose \times B.W. / 1000} \times 100 \quad \text{(Eq.5)}$$

%injectedDose represents the percentage of injected lipid dose taken up into the tissues. LipidAmount is the lipid amount taken up into the whole tissue (liver or spleen) in mg, and B.W. is the body weight of mouse in grams. LipidDose represents the lipid dose for I.V. injection in mg/kg.

VIII. Data Analysis

The drug release half-lives from liposomes *in vitro* were estimated by fitting the data with an exponential decay model. Pharmacokinetic parameters of the total DB-67 (lactone and carboxylate) plasma concentrations and lipid plasma concentration were estimated using a non-compartmental approach (WinNonlin v.5.2). For the estimation of the total AUCs and the errors of plasma samples obtained destructively, Bailer's method [Bailer 1988] was used as described below for a number of discrete samples ranging from i =1 (for the sample collected at the first time point) to i=m (for the sample collected at the last time point).

$$AUC_0^t = \sum_{i=1}^{m} w_i \overline{C}_i \,,$$

Where w is a weighting factor calculated as follows:

$$w_i = \frac{1}{2}(t_2 - t_1) \text{, if } i=1$$

$$= \frac{1}{2}(t_{i+1} - t_{i-1}) \text{ , if } i=2 \text{ to } i=m\text{-}1$$

$$= \frac{1}{2}(t_m - t_{m-1}) \text{, if } i=m$$

$\overline{C}_i$ is the mean of concentration values at the i^{th} sampling time. Concentrations below the limit of quantification were zeroed. The variance of the AUC estimate is calculated as follows:

$$Var[AUC] = \sum_{i=1}^{m} \frac{w_i{}^2 s^2{}_i}{n_i}$$

Where n_i=number of animals euthanized at the i^{th} sampling time and s_i^2 is the variance of plasma or tissue concentration at the i^{th} sampling time. Confidence intervals for AUCs were calculated as follows:

$$AUC \pm t_{\left(\frac{1-\alpha}{2}\right)} df \sqrt{Var(AUC)}$$

The degree of freedom (*df*) for the t-distribution was calculated by Bailer-Satterthwaite's approximation [Nedelman et al. 1995].

$$df = \frac{(\sum_{i=1}^{m} \frac{w_i{}^2 s^2{}_i}{n_i})^2}{\sum_{i=1}^{m} wi^4 s_i{}^4 / n_i{}^2 (n_i - 1)}$$

For the estimation of the errors on clearance, Delta's method [Agresti 1990] was used as described below.

Suppose Y is a random variable and we know the variance of Y, denoted as Var(Y). We have a function of Y, denoted as f(Y). Then, the variance of function Y, denoted as Var[f(Y)], can be calculated by the following equation:

$$Var[\ f(Y)] = [f\ '\ (Y)]^2 * Var(Y)$$

Where f ' (Y) is the derivative of function Y, f(Y).

Statistical tests were performed by GraphPad Prism v5.0 (GraphPad Software, La Jolla, CA). All the plots were made with GraphPad Prism v5.0.

Chapter Four Results

I. Cholesterol, Drug-to-lipid Ratio and Particle Size Effects on DB-67 Release *in Vitro*

The first set of experiments were aimed at characterizing the influence of cholesterol content, drug-to-lipid (D/L) ratio and particle size on DB-67 release rate from liposomes. Cholesterol free liposomes (DSPC:m-PEG-DSPE 95:5 mole %) and cholesterol containing liposomes (DSPC:Chol:m-PEG-DSPE 55:40:5 mole %) were made via an extrusion method as indicated under *Methods*. DB-67 was loaded into liposomes at the drug-to-lipid ratio of 0.03 or 0.3 (w:w). In order to determine the drug release kinetics in the conditions similar to that *in vivo*, the DB-67 entrapped liposomes were dialyzed against a simulated buffer (C-PBS, pH 7.4, 298 mOsm) at 37°C. As shown in Figure 4.1, liposomes without cholesterol retained the drug longer as compared to cholesterol containing liposomes ($p=0.001$, Two-way ANOVA), and DB-67 was retained in the liposomes for a longer period of time at the lower level of drug-to-lipid ratio (0.03, w:w) than that at the higher level (0.3, w:w) regardless of lipid composition ($p<0.0001$, Two-way ANOVA). The drug release half-lives and the release rate constants are shown in Table 4.1 and the detailed statistical analysis results are shown in Appendix I.

The effect of particle size on DB-67 release was investigated with a similar *in vitro* dialysis assay, using cholesterol free liposomes loaded at a drug-to-lipid ratio of 0.3 (w:w). Liposomes were made with particle size of 103±15 nm and dialyzed against C-PBS (pH 7.4, 298 mOsm) at 37^{o}C for 24 hr. The release half-life of DB-67 from liposomes with particle size of 146±40 nm was determined by Joguparthi [Joguparthi 2007]. The release rate constant for 146 nm liposomes was 0.06±0.004 as compared to 0.104±0.007 1/hr for 103 nm liposomes, so DB-67 was retained longer in larger liposomes ($p=0.0005$, *t* test). The release half-lives are shown in Figure 4.2.

The proceeding results indicated that the effect of cholesterol incorporation (40 mole %) was to increase DB-67 release rate about 2 times at the drug-to-lipid ratio of 0.03 (w:w) and that DB-67 was retained 1.7-fold longer in 146 nm liposomes than 103 nm liposomes. But the pharmacokinetic properties of these formulations need to be further evaluated *in vivo* because: 1) the same effects of cholesterol and particle size are not necessarily held when the drug gets into the body; and 2) the pharmacokinetics of liposome associated drug not only depends on the drug release rates from the liposomes, but also relies on the pharmacokinetics of the liposomal carrier itself [Drummond et al. 2008]. The following studies were aimed at determining the effects of cholesterol and particle size on pharmacokinetics of liposomal DB-67. A 2×2 factorial experiment was designed with cholesterol content (40 vs. 0 mole %) and particle size (~180 vs. ~120 nm) being the two factors.

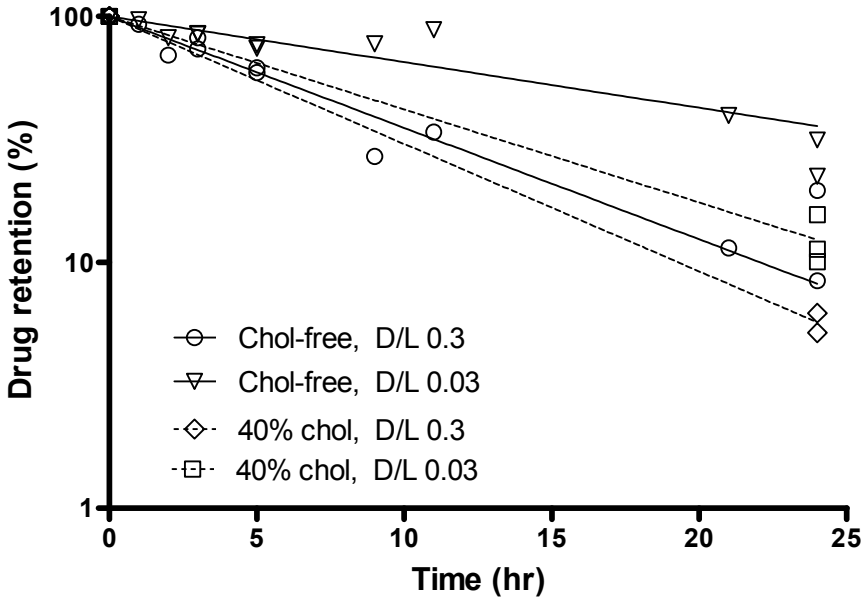

Figure 4. 1 The effects of drug-to-lipid (D/L) ratio and cholesterol content on the retention of DB-67 in liposomes *in vitro*.
DB-67 loaded liposomes were dialyzed against C-PBS (pH 7.4, 298 mOsm) at 37°C for 24 hr. Symbols represent observed data and the lines represent the fitting of the data with an exponential decay model. The particle size of liposomes ranged from 103 to 121 nm.

Table 4. 1 DB-67 release half-lives and the release rate constants from various liposomes. DB-67 loaded liposomes were dialyzed against C-PBS (pH 7.4, 298 mOsm) at 37°C for 24 hr. The drug release half-lives and the release rate contents were determined by fitting the data with an exponential decay model.

Chol level (mole %)	D/L ratio*	Release rate constant (1/hr)	Half-life (hr)
0	0.03	0.043 (0.032 -0.054)	16.22 (12.85 - 21.99)
0	0.3	0.104 (0.089 - 0.119)	6.64 (5.81 - 7.76)
40	0.03	0.087 (0.078 - 0.096)	7.95 (7.19 - 8.90)
40	0.3	0.119 (0.114 - 0.125)	5.81 (5.56 - 6.08)

*D/L ratio: drug-to-lipid ratio

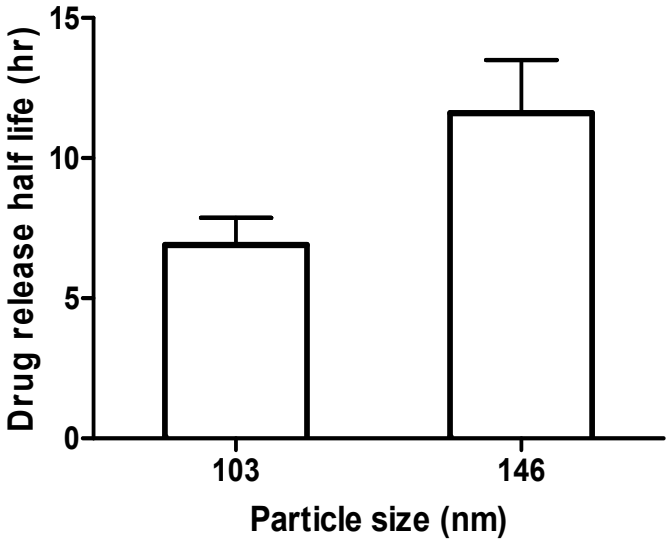

Figure 4. 2 The effect of particle size on the *in vitro* release half-life of DB-67.
DB-67 loaded liposomes were dialyzed against C-PBS (pH 7.4, 298 mOsm) at 37°C for 24 hr and the drug release half-lives were calculated by fitting the data with an exponential decay model. The liposomes used in this experiment were cholesterol free (DSPC:m-PEG-DSPE 95:5 mole %) and the drug-to-lipid ratio was 0.3 (w:w). The data from 146 nm particle size liposomes were adopted from Joguparthi's thesis (Chapter eight, Table 8.3) [Joguparthi 2007].

II. Particle Size and Cholesterol Effects on Lipid Clearance *in Vivo*

The liposomes were injected intravenously into mice at a dose of ~250 mg/kg lipid. The DB-67 dosage in these experiments ranged from 0.3 - 1.3 mg/kg. A mild interaction was observed between particle size and cholesterol content effects on the lipid clearance ($p=0.049$, Two-way ANOVA), and the detailed statistical analysis is shown in Appendix I. The liposomal pharmacokinetics in blood (Figure 4.3) showed that smaller particles persisted in the circulation longer than larger particles ($p=0.0002$, Two-way ANOVA). The lipid clearance of ~180 nm liposomes was 1.8-fold higher than that of ~120 nm liposomes. The effect of cholesterol content on lipid clearance was minimal ($p=0.268$, Two-way ANOVA). Pharmacokinetic parameter estimates for the data shown in Figure 4.3 are presented in Table 4.2.

III. Particle Size and Cholesterol Effects on DB-67 Clearance *in Vivo*

In the same experiments, as depicted in Figure 4.3, DB-67 concentration was assayed by a validated fluorescence HPLC assay. These measurements represented the liposomal and free drug concentrations for both lactone and carboxylate in the plasma. Dose normalized plasma DB-67 concentration versus time profiles are shown in Figure 4.4. Overall, DB-67 was cleared faster from the circulation in larger particles than the smaller ones ($p<0.0001$, Two-way ANOVA). Specifically, DB-67 clearance was about 2-fold higher in ~180 nm liposomes than that in ~120 nm liposomes when cholesterol was present (Figure 4.4 B).

Incorporation of cholesterol (40 mole %) in the liposomes led to an increase of DB-67 clearance of 1.5-fold and 2.9-fold in ~120 nm and ~180 nm particle size of liposomes, respectively ($p<0.0001$, Two-way ANOVA). The increased DB-67 clearance caused by cholesterol incorporation can be partially due to the elevated DB-67 release rate from cholesterol containing liposomes, as compared to that from cholesterol free liposomes (Figure 4.1). Once DB-67 was released from liposomes, it was cleared faster than the liposome associated DB-67 [Joguparthi and Anderson 2008], so the elevated drug release rate directly led to increased clearance of DB-67. Pharmacokinetic parameter estimates for the data shown in Figure 4.4 are presented in Table 4.3.

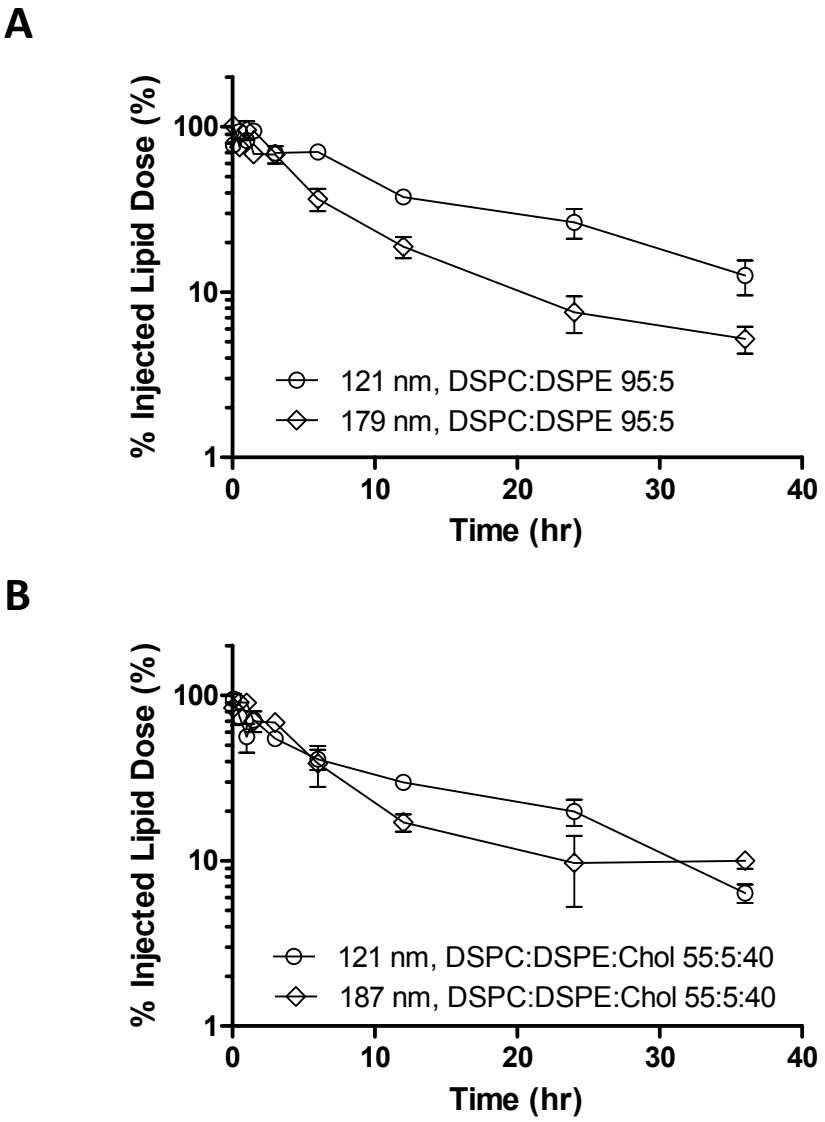

Figure 4. 3 Pharmacokinetics of liposomes in the blood.
Liposomes radiolabeled with [^{3}H]-CHE were administered intravenously in the lateral tail vein to female C57/BL6 mice. Particle size effects on lipid elimination were shown in cholesterol free (A) and cholesterol containing liposomes (B). Data were the average percentage of injected lipid dose remaining in the circulation ±S.D. for three mice at each time point.

Table 4. 2 Pharmacokinetic parameter estimations of lipid in mice after intravenous injection of various liposomal formulations. Liposomes were prepared with 40% (molar ratio) or without cholesterol in two different sizes (~120 nm and ~180 nm). Data are shown as mean ± S.E.

Cholesterol Content (mole %)	**Particle Size** (nm)	**Lipid Dose** (mg/kg)	**V**[b] (ml/kg)	**AUC**[a] (hr*mg/ml)	**CL**[a] (ml/hr/kg)	**$T_{1/2}$**[b] (hr)
0	121±18	234.5	40.15	105.34±5.87	2.23±0.12	15.19
0	179±21	255.9	56.60	64.08±3.87	3.99±0.24	10.76
40	121±17	235.8	45.71	76.54±4.09	3.08±0.16	11.63
40	187±23	240.1	71.81	64.16±5.92	3.74±0.35	16.41

V: Apparent volume of distribution
AUC: Area under the plasma concentration-time curve from time zero to 36 hr
CL: Apparent clearance
$T_{1/2}$: elimination half-life
[a] Pharmacokinetic parameters were estimated by Bailer Method (see details in Method section)
[b] Pharmacokinetic parameters were estimated by non-compartmental analysis

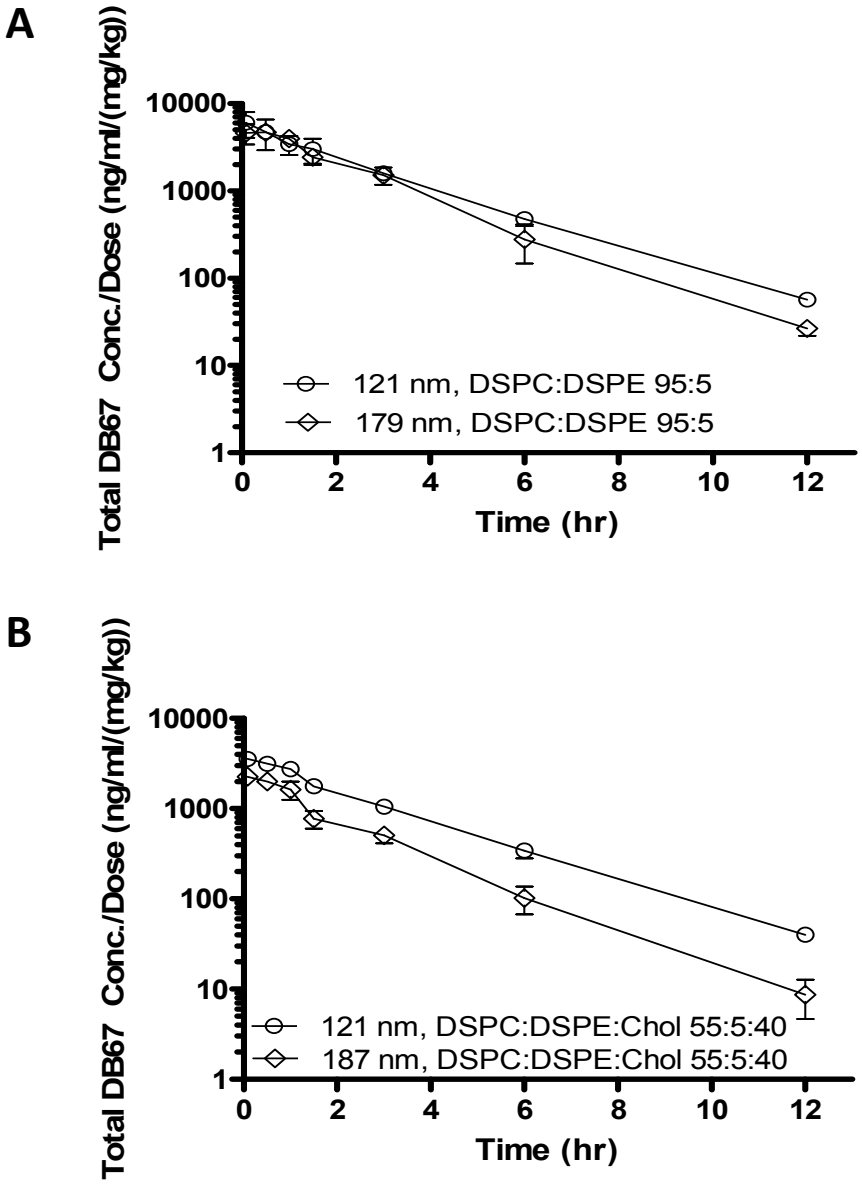

Figure 4. 4 Pharmacokinetics of liposomal DB-67 in the blood.
Liposomes radiolabeled with [^{3}H]-CHE and loaded with DB-67 were administered intravenously in the lateral tail vein to female C57/BL6 mice. Dose normalized total DB-67 (both lactone and carboxylate of encapsulated and fee drug) plasma concentrations were shown in cholesterol free liposomes (A) and cholesterol containing liposomes (B). Data were the average plasma DB-67 concentration normalized by DB-67 dose in the circulation ±S.D. for three mice at each time point.

Table 4. 3 Pharmacokinetic parameter estimates of liposomal DB-67 in mice after intravenous injection of various liposomal formulations.
Liposomal DB-67 was prepared with 40% (molar ratio) or without cholesterol in two different particle sizes (~120 nm and ~180 nm). Data are shown as mean ± S.E.

Cholesterol Content (mole%)	**Particle Size** (nm)	**Lipid Dose** (mg/kg)	**DB-67 Dose** (mg/kg)	**V[b]** (ml/kg)	**AUC[a]** (hr*μg/ml)	**CL[a]** (ml/hr/kg)	**$T_{1/2}$[b]** (hr)
0	121±18	234.5	1.34	180.84	19.29±0.19	69.46±4.27	1.84
0	179±21	255.9	1.36	166.87	17.97±0.94	75.70±3.97	1.57
40	121±17	235.8	0.24	279.01	2.33±0.05	103.10±2.37	1.91
40	187±23	240.1	1.07	472.26	4.93±0.24	216.87±10.53	1.55

V: Apparent volume of distribution
AUC: Area under the plasma concentration-time curve from time zero to 36 hr
CL: Apparent clearance
$T_{1/2}$: elimination half-life
[a] Pharmacokinetic parameters were estimated by Bailer Method (see details in Method section)
[b] Pharmacokinetic parameters were estimated by non-compartmental analysis

IV. Particle Size and Cholesterol Effects on Tissue Uptake of Liposomes

The effect of cholesterol and particle size on the liver and spleen uptake, which represent the major liposome clearance pathways, were also determined *in vivo*. Mice were injected with liposomes as described in the *Method*s section. The liver and spleen were collected and [^{3}H]-CHE was measured via a scintillation counting method. Liposomes with smaller particle size (~120 nm) were taken up to a lesser extent by the liver and spleen than the larger liposomes (~180 nm) (Figure 4.5). At 24 hr post injection, about 45.1±3 % and 30.3±4 % of injected lipid dose was present in the liver for ~180 nm and ~120 nm particle size liposomes, respectively (p=0.006, *t* test). In the spleen, 13.2±3 % of injected lipid dose was accumulated for ~180 nm particle size liposomes as compared to 6.2±1 % for ~120 nm liposomes at 24 hr after injection (p=0.011, *t* test). The decreased tissue uptake of smaller liposomes correlates with the longer circulation of these liposomes in blood (see Figure 4.3).

Cholesterol, on the other hand, did not affect the tissue uptake of liposomes (Figure 4.5). On average, about 36.8 – 49.3 % of injected lipid dose was accumulated in the liver for cholesterol free liposomes as compared to 36.3 – 39.2 % for cholesterol containing liposomes and the difference is not significant at the time points observed (p=0.945 at 12h post-dose, p=0.052 at 24h post-dose, p=0.062 at 36h post-dose, *t* test). In the spleen, averagely, about 13.3 – 14.7 % and 11.7 – 15.2 % of injected liposomal dose was present for cholesterol free liposome and cholesterol containing liposome, respectively and the effect is not significant either (p=0.550 at 12h post-dose, p=0.504 at 24h post-dose, p=0.909 at 36h post-dose, *t* test). These biodistribution data were consistent with the liposomal pharmacokinetics in the blood, which demonstrated that cholesterol had minimal effect on liposomal clearance.

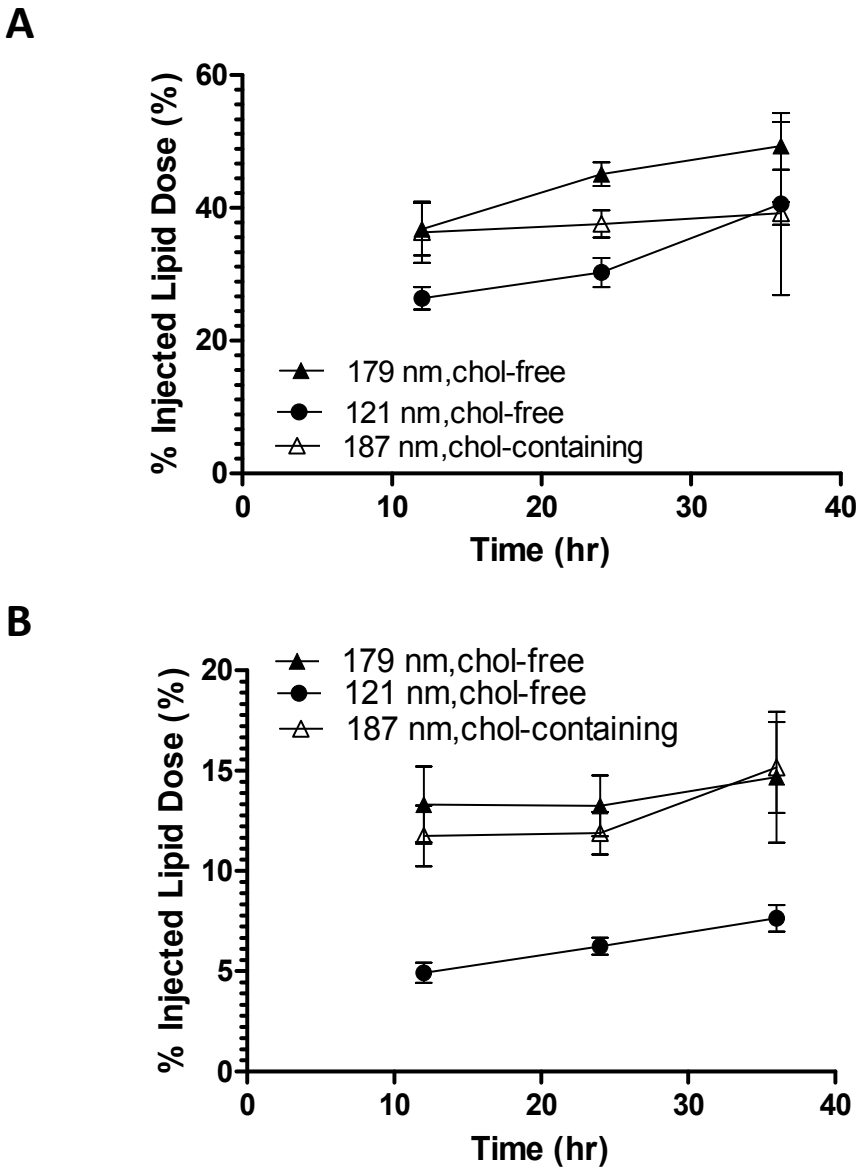

Figure 4. 5 Liposomal biodistribution of various liposomal formulations.
Liposomes radiolabeled with [^{3}H]-CHE were administered intravenously in the lateral tail vein to female C57/BL6 mice. The liver and spleen tissues were collected and the radioactivity was measured. The effects of particle size and cholesterol on tissue uptake of liposomes were shown in liver (A) and spleen (B). Data were the average percentage of injected lipid dose accumulated in the tissue ±S.D. for three mice at each time point.

V. Liposomal Dose Effect on Lipid Clearance, DB-67 Clearance and Tissue Uptake

The studies described thus far demonstrated that cholesterol free liposomes with particle size of ~120 nm had the extended circulation half-life and the minimum DB-67 clearance. Therefore, we used this particular formulation to examine the effect of lipid dose on the clearance of lipid and DB-67. Liposomal DB-67 was injected into mice with lipid doses of 63.6, 234.5, and 703.9 mg/kg and DB-67 doses of 0.30, 1.34, and 3.35 mg/kg, correspondingly. The percentage of injected lipid dose versus time and the dose normalized plasma DB-67 concentration versus time profiles are shown in Figure 4.6 A and Figure 4.6 B, respectively. When the lipid dose was increased from 64 to 704 mg/kg, a reduction of lipid clearance from 2.4±0.2 to 1.6±0.03 ml/h/kg (1.5-fold decrease, $p=0.0012$, ANOVA) was observed. Accordingly, a drop of DB-67 clearance from 96.4±7.8 to 28.2±1.6 ml/h/kg ($p<0.0001$, ANOVA), and an increase in DB-67 elimination half-life from 1.8 to 2.5 hr were obtained. The reduced DB-67 clearance associated with higher liposomal doses can be partially explained by the decreased clearance of liposomal carriers from the blood.

The elimination profile of non-liposomal DB-67 was compared with those from liposomal DB-67 in Figure 4.6 B. Mice receiving the lowest lipid dose (64 mg/kg) were exposed to a 40-fold higher DB-67 AUC (dose normalized), and had a 2.8-fold increase of elimination half-life as compared to those received non-liposomal DB-67. The DB-67 clearance was 3323.4±424.1 ml/hr/kg when administered in non-liposomal formulation as compared to 96.4±7.8 ml/hr/kg in liposomal formulation (at the lipid dose of 64 mg/kg). The terminal elimination half-life was prolonged from 0.62±0.11 hr for free DB-67 to 1.8 hr for liposomal DB-67. Pharmacokinetic parameter estimates for the data shown in Figure 4.6 A and Figure 4.6 B are presented in Table 4.4 and 4.5, respectively.

In the same experiments the liver and spleen tissues were collected at 12, 24 and 36 hr and [3H]-CHE in the tissues was measured via scintillation counting. The percentages of injected lipid dose accumulated in the tissues are shown in Figure 4.7 A (liver) and Figure 4.7 B (spleen). The accumulation of liposomes was higher at the two larger levels of lipid doses but the effect was not statistically significant ($p=0.16$ in the liver, $p=0.08$ in the spleen, ANOVA). The slightly higher levels in tissues of mice administered the 234.5mg/kg lipid dose suggest that this dose may be close to saturating the RES.

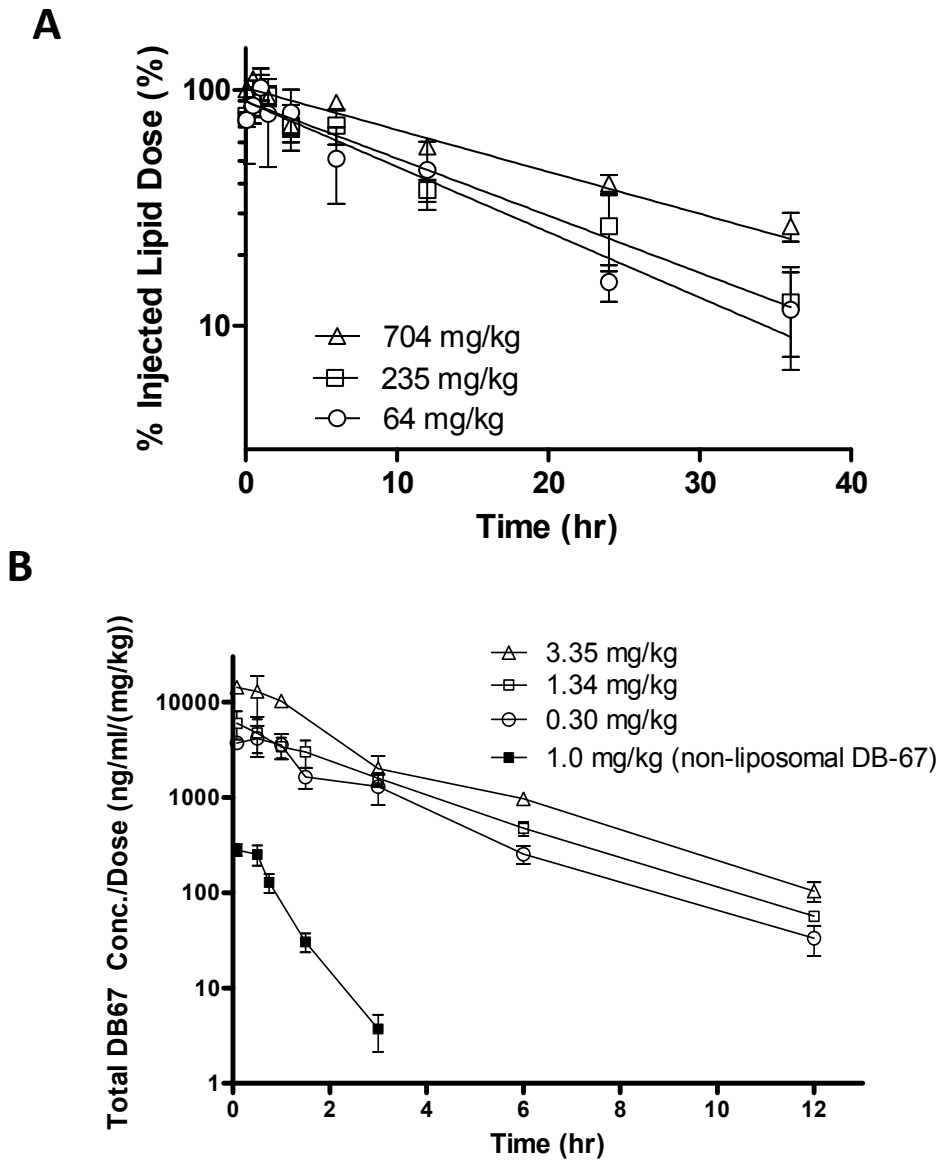

Figure 4. 6 The effect of lipid dose on the pharmacokinetics of liposomes and liposomal DB-67. Liposomal DB-67 radiolabeled with [^{3}H]-CHE or non-liposomal DB-67 was administered intravenously in the lateral tail vein of female C57/BL6 mice. Data were the percentage of injected lipid dose remained in the blood (A, lines represent the fit of the data with a one compartment exponential decay model) and the dose normalized total DB-67 (both lactone and carboxylate of encapsulated and fee drug) concentration in the plasma (B). Each data point represented the average value ±S.D. for three mice at each time point.

Table 4. 4 Pharmacokinetic parameter estimations of lipid in mice after intravenous injection of liposomal DB-67 at various lipid doses.
Cholesterol free liposomes radiolabeled with [^{3}H]-CHE were prepared and injected at lipid doses of 64 to 704 mg/kg. Data are shown as mean ± S.E.

Lipid Dose (mg/kg)	**Particle Size** (nm)	**V**[b] (ml/kg)	**AUC**[a] (hr*mg/ml)	**CL**[a] (ml/hr/kg)	**$T_{1/2}$**[b] (hr)
63.6	103±11	45.05	26.41±2.12	2.41±0.19	16.31
234.5	121±18	40.15	105.34±5.87	2.23±0.12	15.19
703.9	115±16	31.44	437.54±8.42	1.61±0.03	18.36

V: Apparent volume of distribution
AUC: Area under the plasma concentration-time curve from time zero to 36 hr
CL: Apparent clearance
$T_{1/2}$: elimination half-life
[a] Pharmacokinetic parameters were estimated by Bailer Method (see details in Method section)
[b] Pharmacokinetic parameters were estimated by non-compartmental analysis

Table 4. 5 Pharmacokinetic parameter estimations of DB-67 in mice after intravenous injection of liposomal DB-67 at various lipid and DB-67 doses. DB-67 was loaded to cholesterol free liposomes radiolabeled with [^{3}H]-CHE. Liposomal DB-67 was injected at the lipid doses of 64 to 704 mg/kg and DB-67 doses of 0.3 to 3.35 mg/kg. Data are shown as mean ± S.E.

Lipid Dose (mg/kg)	**DB-67 Dose** (mg/kg)	**Particle Size** (nm)	**V**[b] (ml/kg)	**AUC**[a] (hr*µg/ml)	**CL**[a] (ml/hr/kg)	**T $_{1/2}$**[b] (hr)
63.6	0.30	103±11	246.79	3.11±0.25	96.39±7.83	1.80
234.5	1.34	121±18	180.84	19.29±1.19	69.46±4.27	1.84
703.9	3.35	115±16	97.94	118.79±6.57	28.2±1.56	2.49

V: Apparent volume of distribution
AUC: Area under the plasma concentration-time curve from time zero to 36 hr
CL: Apparent clearance
$T_{1/2}$: elimination half-life
[a] Pharmacokinetic parameters were estimated by Bailer Method (see details in Method section)
[b] Pharmacokinetic parameters were estimated by non-compartmental analysis

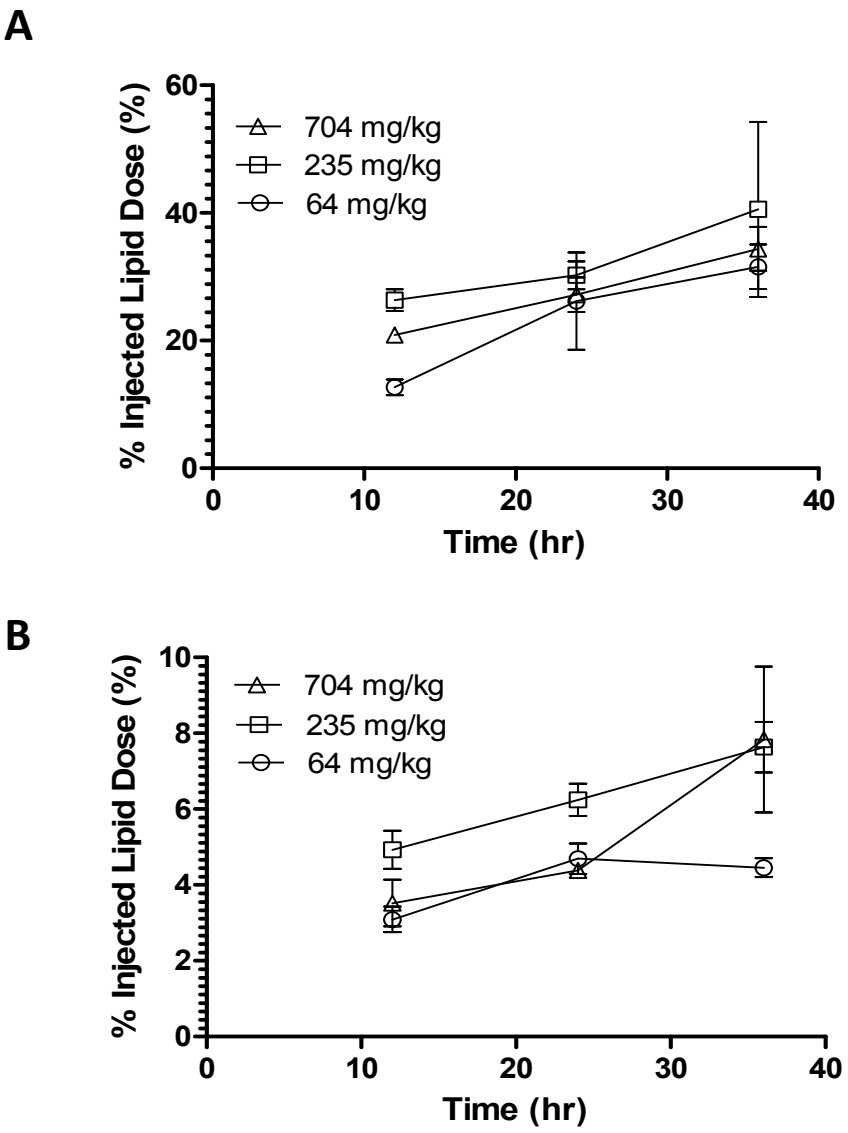

Figure 4. 7 The effect of lipid dose on the biodistribution of DB-67 loaded liposomes.
DB-67 loaded liposomes radiolabeled with [^{3}H]-CHE were administered intravenously in the lateral tail vein of female C57/BL6 mice. The liver and spleen tissues were collected and the radioactivity was measured by scintillation counting. Data were the percentage of injected lipid dose accumulated in the liver (A) and spleen (B). Each data point represented the average value ±S.D. for three mice at each time point.

Chapter Five Discussion

The ultimate goal of developing a liposomal formulation for a given anti-cancer agents is to enhance its anti-tumor efficacy and to minimize its toxicity. This requires the development of formulations that have appreciable amounts of liposomes circulating in plasma for at least 24 hours. Implicitly this also requires that the release rate of drug from liposomes is no lower than the rates that define liposome clearance from the systemic circulation [Drummond et al. 2008]. The liposomal formulation can be optimized by controlling the factors influencing these two processes. Cholesterol, particle size and lipid dose are the three critical factors evaluated in the development of liposomal DB-67 in our study. The present experiments demonstrate that liposomes with particle size of ~120 nm provide longer DB-67 elimination half-life. Furthermore, cholesterol free liposomes of such particle size exhibit the slowest DB-67 release rate and have the lowest DB-67 clearance. Therefore, we chose the particle size of ~120 nm and cholesterol free liposomes as the formulation of liposomal DB-67 for further development. In addition, the higher lipid dose further decreases liposomal clearance. However, while the higher lipid dosages can impair RES mediated liposomal clearance, toxicities associated with high lipid doses, such as hepatomegaly and granulomas [Allen et al. 1984], will have to also be considered. The effects of the formulation factors on the pharmacokinetics of liposomes and liposomal DB-67 are discussed further below.

I. Factors that Influence Pharmacokinetics of Liposomes

Our studies have shown that the larger particle size leads to shorter elimination half-life of liposomes. This result is consistent with the findings of previous studies. Woodle et al. reported that the blood levels of lipid at 24 hr showed a decrease from more than 20% to about 10% of the injected dose when the mean particle diameter was increased from 100 to 200 nm [Woodle et al. 1992]. The size dependence of liposomal pharmacokinetics is even more striking when the liposome is not sterically stabilized [Drummond et al. 1999]. DSPC:Chol (3:2 molar ratio) liposomes with size of 400 nm are cleared 7.5 time as fast as liposomes of 200 nm, which are cleared 5-time faster than smaller liposomes [Senior et al. 1985]. However, liposomes that are smaller than 100 nm are cleared faster than those that are between 100 - 200 nm. Thus, it appears that the smaller physical size is required to evade the RES but smaller paticles have a greater surface area for the same lipid dose, resulting in more plasma protein binding per liposome. Since plasma protein binding facilities liposomal clearance, higher protein binding (opsonization) leads to faster clearance of these smaller size liposomes. It is also worth noting that we loaded active drug (DB-67) into the liposome, whereas Woodle et al. applied blank liposome without any drug [Woodle et al. 1992]. The similarity of the half-lives in both studies indicates that DB-67 does not alter the

pharmacokinetic properties of the liposomal carriers dramatically. However, this is not always the case. As shown by Li et al., encapsulated vincristine significantly affected the pharmacokinetics of liposomes in mice [Li et al. 1998]. This suggests that one has to examine the *in vivo* pharmacokinetics of liposomes containing entrapped drug of interest to optimize the formulation, and it is unlikely to have a generic liposomal formulation that suits all the anti-tumor agents.

The impact of cholesterol on liposomal clearance is assessed in the present study and it is shown that cholesterol containing liposomes exhibit circulation lifetime comparable to those of cholesterol free liposomes. Dos Santos et al. demonstrated similar results. Namely, about 29% of the injected dose was present in the circulation after 24 hr for both cholesterol free and cholesterol containing liposomes [Dos Santos et al. 2002]. Woodle et al. also reported that PEG-PE:PC:Chol (1:10:5 molar ratio, PC refers to PHEPC IV 40 partially hydrogenated egg phosphatidylcholine with iodine values from 1 to 40 and PEG-PE to ^{1900}PEG-DSPE) and PEG-PE:PC (0.15:1.85 molar ratio) liposomes showed similar elimination half-lives of 15.8 and 14.7 hr, respectively [Woodle et al. 1992]. Nevertheless, others concluded that cholesterol was required to maintain the stability of liposomes in the plasma [Damen et al. 1981; Kirby et al. 1980]. For instance, Semple and Chonn demonstrated that the elimination half-life was 5 hr for liposomes containing 30 mole % cholesterol as compared to seconds for liposomes without cholesterol and that this was mainly due to reduced protein binding to the cholesterol containing liposomes [Semple et al. 1996]. The divergence we see here is attributed to the surface stabilizing compounds, PEG, which we and Woodle et al. applied. It is believed that PEG minimizes liposome-liposome aggregation by providing a strong steric barrier even with as little as 0.72 mole % in the liposome composition [Klibanov et al. 1991]. Additionally, it may also inhibit protein binding by shielding defects on the surface of liposomes [Dos Santos et al. 2002], thereby preventing them from recognition by opsonizing plasma proteins.

Liposomal dose influences liposome elimination in the blood and an inverse relationship between the liposome dose and the lipid clearance is observed for conventional liposomes [Allen and Hansen 1991; Oja et al. 1996]. Oja et al. reported that when the liposome dose was increased from 50 to 500 mg/kg, the percentage of injected lipid dose remained in the circulation at 12 hr post injection was dramatically enhanced from 4 to 58 %. It is proposed that there is a limited pool of blood proteins that is able to bind to liposomes. When greater amount of liposomes is administered (high liposomal doses), the blood protein which can bind to the liposomes is diluted over a larger surface area. Therefore, the amount of blood protein bound per liposome is reduced as compared to low liposomal doses, in turn, resulting longer circulation lifetime of these liposomes [Oja et al.

1996]. Another explanation for the dose effect on liposome clearance is binding site saturation in the RES at higher liposome doses [Allen and Hansen 1991]. Liposomes are thought to be taken up by macrophages of the RES, the saturation of the macrophages leads to decreased liposomal clearance rates at higher liposomal doses. In the present study, we also observe the same trend, but it is not as dramatic as the previous studies. With about 10-fold increase of liposome dose (64 to 704 mg/kg), the percentage of injected lipid dose remained in the circulation at 24 hr is increased from 15±3 % to 40±3 %. The circulation lifetime enhancement associated with the higher liposome doses is diminished in our study because we use "sterically stabilized" liposomes instead of the conventional liposomes (DSPC:Chol 55:45 mole %) used elsewhere [Allen and Hansen 1991; Oja et al. 1996]. For this particular liposomal DB-67 formulation, liposomal clearance is less dependent on the lipid dose, which simplifies the pharmacokinetics and provides further advantages for the clinical development of this formulation.

II. Factors that Influence Pharmacokinetics of Liposomal DB-67

The increase of particle size leads to an increase of liposomal DB-67 clearance. In our study, liposomal carriers are eliminated more quickly from the blood in larger particles than in the smaller ones. However, the *in vitro* DB-67 release rate from the liposomes is higher in smaller particle size liposomes (see Figure 4.2). These two effects oppose to each other, but the combined effect *in vivo* is reflected as the pharmacokinetics of liposome-associated DB-67. With the increase of particle size, the clearance of liposomal DB-67 is increased (see Figure 4.4). It reveals that the clearance of liposomal carriers is a dominant process here. Therefore, we choose smaller particle size liposomes (~120) in the development of the formulation.

Cholesterol incorporation (40 mole %) results in an increase of liposomal DB-67 clearance which can be attributable to the increased DB-67 release from cholesterol containing liposomes as compared to that from cholesterol free ones. At 37°C, liposomes composed of DSPC: m-PEG DSPE (95:5 mole %) are in solid gel phase. However, when 40 mole % of cholesterol is incorporated, liposomal membrane is in the transition state from solid gel to liquid crystalline phase, which is more permeable [Xiang and Anderson 1997]. So, DB-67 is released 2 times faster from cholesterol containing liposomes than from liposomes without cholesterol (Figure 4.1), and it leads to the higher clearance of liposomal DB-67 from the circulation. Overall, the effect of cholesterol on the clearance of liposomal drug is complicated because it depends on both the specific drug applied and the lipid membrane composition. In the early studies, liposomes composed of high cholesterol content (>33 mole%) were used in the liposomal drug delivery since they demonstrated the longest drug retention *in vivo* [Ogihara-Umeda and Kojima 1989]. Then in 2002, Dos Santos

et al. showed that the maximum retention of idarubicin was achieved using cholesterol free liposomes. The AUC $_{0\text{-}24h}$ from idarubicin encapsulated in the liposomes was 45-fold higher than that from the free drug [Dos Santos et al. 2002]. It was postulated that the greater drug retention associated with cholesterol free liposomes was attributed to the enhanced interaction of lipid membrane to idarubicin [Dos Santos et al. 2002]. More interestingly, in a study by Tardi et al., an opposite effect of cholesterol on drug retention was observed in the two drugs simultaneously entrapped into the liposomes - floxuridine was retained dramatically longer in cholesterol free (DSPC : distearoylphosphatidylglycerol (DSPG) 8:2, mol/mol) liposomes (16 hr vs. 1 hr) whereas, irinotecan was released 5-fold faster in cholesterol free liposomes (10 mole %) [Tardi et al. 2007]. In the present study, we choose cholesterol free liposomes as the optimal lipid composition because it has the lowest DB-67 clearance from the blood.

III. Factors that Influence Tissue Uptake of Liposomes

This study shows that liposomes with the particle size of 180 nm are taken up more extensively by the liver and spleen than the 120 nm liposomes. This is in agreement with a study by Woodle et al., wherein about 25% of injected liposome dose was accumulated in the liver and spleen for 150 nm liposomes as compared to only 7% for 100 nm liposomes (in rats) [Woodle et al. 1992]. It is widely believed that the tissue uptake of liposomes depends on the particle size. Large particle size liposomes (d>200 nm) are quickly filtered from the circulation by the spleen [Ishida et al. 1999; Litzinger et al. 1994]. On the other hand, very small liposomes (d<70 nm) are accumulated most in liver and are localized in Kupffer cells [Litzinger et al. 1994]. Our study compared the size-dependence of tissue uptake of liposomes within a narrower range (100 to 200 nm). The exact mechanism driving the greater accumulation of ~180 nm liposomes in the RES than ~120 nm liposomes needs to be further investigated.

In our study, cholesterol does not have significant effect on the tissue uptake of liposomes, even though it was reported by Ogihara-Umeda and Kojima that a large amount of cholesterol (>33 mole %) leads to a decrease in the uptake of liposomes by the liver and spleen [Ogihara-Umeda and Kojima 1989]. It is noteworthy that, firstly, they used conventional liposomes, and we used sterically stabilized liposomes; secondly, the less tissue uptake of cholesterol containing liposomes was only observed at 1 hr after the injection in their study. At 24 hr, the liposome tissue uptake was very similar regardless of the cholesterol content, with 21.0 % of injected lipid dose accumulated in the liver and spleen for cholesterol free liposomes as compared to 22.0 % for cholesterol containing liposomes.

The present study shows that the RES uptake of liposomes is comparable in the lipid dose range of 64 to 704 mg/kg and about 31±11 %, 36±4%, and 32±5 % of the injected lipid dose is taken up by the RES at 24 hr post injection for the low, middle and high lipid doses, respectively. However, it was demonstrated in other liposomal systems that with the increase of lipid dose, the RES uptake of liposomes decreases, as reflected by the reduction of the percentage of injected lipid dose accumulated in those tissues [Allen and Hansen 1991; Oja et al. 1996]. For example, 61% of the injected lipid dose was recovered in the RES at the high lipid dose (10.0 μmol phospholipid/mouse) at 48 hr post injection as compared to 80% for the low lipid dose (0.1 μmol/mouse, lipid composition PC:Chol 2:1 molar ratio) [Allen and Hansen 1991]. Nevertheless, the observations in sterically stabilized liposomes are distinctly different. In the same study, it was shown that the RES tissue uptake of "stealth" liposomes averaged 27% at 24 hr post injection for the lipid dose ranged from 0.1 to 10 μmol/mouse [Allen and Hansen 1991]. Overall, the RES uptake of liposomes is dramatically reduced in "stealth" liposomes than that in conventional liposomes. It is because that the steric barrier formed by GM1 or PEG significantly reduces the protein binding to the liposomes, which subsequently decreases the RES uptake. The barrier also diminishes the dose-dependence of the liposomal tissue uptake. Furthermore, the less extent of RES uptake of the "stealth" liposomes decreases the toxicities of the liposomes arising from the RES impairment.

Chapter Six Conclusions

The work presented in this thesis is designed to characterize the drug release and pharmacokinetics of liposomal DB-67. The sterically stabilized liposomes, with saturated lipid as the major component (DSPC:mPEG-DSPE 95:5 mole%), is applied. Factors influencing DB-67 release and pharmacokinetics are thoroughly investigated.

In summary, *in vitro* dialysis experiments show that cholesterol incorporation and smaller particle size lead to increased DB-67 release from liposomes and higher drug-to-lipid ratio results in faster DB-67 release. *In vivo*, however, the cholesterol free liposomes with relatively smaller particle size (~120 nm) demonstrate the longer liposomal elimination half-life and the least DB-67 clearance from the circulation. The higher lipid dose prolongs the liposomal elimination half-life and reduces DB-67 clearance further, but considering the RES impairment toxicities related to the high lipid dose, 60 to 100 mg/kg lipid doses may be used in the future development. At this dose range, a 40-fold increase of DB-67 AUC (dose normalized) in the plasma is achieved by using liposomal formulation as compared to the non-liposomal DB-67. Additionally, the larger particle size liposomes (~180 nm) are taken up to the liver and spleen in a greater extent than the smaller liposomes (~120 nm). However, neither the cholesterol content nor the lipid dose alters the tissue uptake of liposomes. Therefore, this liposomal formulation demonstrates the great potential to be applied in DB-67 delivery.

Currently, an active drug loading strategy is undergoing development to improve the encapsulation rate and to further enhance the DB-67 retention in the liposomes. A divalent metal ion may be entrapped into liposomes as a complexing agent, so that the mechanism of drug release is altered from a membrane permeation process to an intravesicular dissolution process. In the future, the anti-tumor efficacy of the liposomal DB-67 will be evaluated in the mouse tumor xenograft models and compared to the non-liposomal formulation. The improved therapeutic index of DB-67 is anticipated to be achieved via the liposomal formulation.

Appendices

Appendix I: Statistical Analysis Results

I. Statistical Analysis of DB-67 Release Rate Constants – the Effects of Cholesterol Content and Drug-to-Lipid (D/L) Ratio on DB-67 Release Rate *in Vitro*

Table 7. 1 ANOVA of drug release rate constants for various formulations of liposomal DB-67

Source of Variation	Degrees of Freedom	Sum of Squares	Mean square
Chol content	1.0	0.005883	0.005883
D/L ratio	1.0	0.01464	0.01464
Interaction	1.0	0.001442	0.001442
Residual (error)	32.0	0.01421	0.0004441
Total	35.0		

Does cholesterol content have the same effect at all values of D/L ratio?

Interaction accounts for approximately 3.99% of the total variance.

F = 3.25. DFn=1 DFd=32

The P value = 0.0810

If there is no interaction overall, there is a 8.1% chance of randomly observing so much interaction in an experiment of this size. The interaction is considered not quite significant.

Does cholesterol content effect the drug release rate constant?

Cholesterol content accounts for approximately 16.26% of the total variance.

F = 13.25. DFn=1 DFd=32

The P value = 0.0010

If cholesterol content has no effect overall, there is a 0.095% chance of randomly observing an effect of this big (or bigger) in an experiment of this size. The effect is considered extremely significant.

Does D/L ratio effect the drug release rate constant?

D/L ratio accounts for approximately 40.46% of the total variance.

F = 32.96. DFn=1 DFd=32

The P value is < 0.0001

If D/L ratio has no effect overall, there is a less than 0.01% chance of randomly observing an effect of this big (or bigger) in an experiment of this size. The effect is considered extremely significant.

II. Statistical Analysis of Lipid Clearance– the Effects of Cholesterol Content and Particle Size on Lipid Clearance *in Vivo*

Table 7. 2 ANOVA of lipid clearance for various formulations of liposomal DB-67

Source of Variation	Degrees of Freedom	Sum of Squares	Mean square
Cholesterol content	1.0	0.5311	0.5311
Particle size	1.0	8.641	8.641
Interaction	1.0	1.785	1.785
Residual (error)	21.0	8.622	0.4106
Total	24.0		

Does cholesterol content have the same effect at all levels of particle size?

Interaction accounts for approximately 9.12% of the total variance.

F = 4.35. DFn=1 DFd=21

The P value = 0.0494

If there is no interaction overall, there is a 4.9% chance of randomly observing so much interaction in an experiment of this size. The interaction is considered significant.

Does cholesterol content affect the lipid clearance?

Cholesterol content accounts for approximately 2.71% of the total variance.

F = 1.29. DFn=1 DFd=21

The P value = 0.2682

If cholesterol content has no effect overall, there is a 27% chance of randomly observing an effect of this big (or bigger) in an experiment of this size. The effect is considered not significant.

Does particle size affect the lipid clearance?

Particle size accounts for approximately 44.13% of the total variance.

F = 21.04. DFn=1 DFd=21

The P value = 0.0002

If particle size has no effect overall, there is a 0.016% chance of randomly observing an effect of this big (or bigger) in an experiment of this size. The effect is considered extremely significant.

III. Statistical Analysis of DB-67 Clearance– the Effects of Cholesterol Content and Particle Size on DB-67 Clearance *in Vivo*

Table 7. 3 ANOVA of DB-67 clearance for various formulations of liposomal DB-67

Source of Variation	Degrees of Freedom	Sum of Squares	Mean square
Cholesterol content	1.0	65710	65710
Particle size	1.0	30970	30970
Interaction	1.0	24860	24860
Residual (error)	31.0	12660	408.5
Total	34.0		

Does cholesterol content have the same effect at all levels of particle size?

Interaction accounts for approximately 19.49% of the total variance.

F = 60.86. DFn=1 DFd=31

The P value is < 0.0001

If there is no interaction overall, there is a less than 0.01% chance of randomly observing so much interaction in an experiment of this size. The interaction is considered extremely significant.

Does cholesterol content affect DB-67 clearance?

Cholesterol content accounts for approximately 48.96% of the total variance.

F = 160.86. DFn=1 DFd=31

The P value is < 0.0001

If cholesterol content has no effect overall, there is a less than 0.01% chance of randomly observing an effect of this big (or bigger) in an experiment of this size. The effect is considered extremely significant.

Does particle size affect DB-67 clearance?

Particle size accounts for approximately 23.08% of the total variance.

F = 75.81. DFn=1 DFd=31

The P value is < 0.0001

If particle size has no effect overall, there is a less than 0.01% chance of randomly observing an effect of this big (or bigger) in an experiment of this size. The effect is considered extremely significant.

Appendix II: Pharmacokinetic Model Selection for Plasma Lipid and DB-67 Disposition

One-compartment and two-compartment models were fitted to the plasma lipid concentration and DB-67 concentration data, and the predicted curves and the weighted residual plots are shown as below for each experiment (Figures 7.1 to 7.6 for plasma lipid disposition and Figures 7.7 to 7.12 for plasma DB-67 disposition). Model selection was based on visual inspection of model fitting and residual plots, and the values of Akaike Information Criterion (AIC), a measure of goodness of fit based on maximum likelihood. When comparing several models for a given data set, the model associated with the smallest AIC is regarded as giving the best fit. AIC value for each model fitting is listed in Table 4.

For liposomes with ~120 nm particle size (regardless of cholesterol content), the lipid disposition can be fitted with one-compartment model based on visual inspection of the model fitting and the weighted residual plots (Figures 7.1, 7.4, 7.5 and 7.6). The AIC values are smaller with one-compartment model fitting as compared to two-compartment (Table 7.4) for ~120 nm particles except for experiments LP-2 and LP-6. But two-compartment models were chosen for experiments LP-2 and LP-6 as the simple model is preferred given that the fitting and residuals were very similar with one or two compartment models, as shown in Figure 7.1 and 7.5.

For liposomes with ~180 nm particle size (regardless of cholesterol content), the lipid disposition can be fitted with two-compartment model based on visual inspection of the model fitting and the weighted residual plots (Figures 7.2 and 7.3). The AIC values are smaller with two-compartment model fitting as compared to one-compartment (Table 7.4).

DB-67 disposition in most of the experiments can be fitted with one-compartment model (except for LP-6) based on visual inspection of the model fitting and the weighted residual plots (Figures 7.7, 7.8, 7.9, 7.10 and 7.12). The AIC values obtained with one-compartment fitting were smaller as compared to two-compartment (Table 7.4). DB-67 disposition in LP-6 can be fitted with a two-compartment model (Figure 7.11). In this experiment, the highest lipid dose (7.4 mg/kg) and DB-67 dose (3.35 mg/kg) were used, so DB-67 concentration was above the lower limit of quantification (LLOQ) at 24 hr. However, the concentration was below LLOQ at 24 hr for the other experiments with lower lipid and DB-67 doses.

Table 7. 4 AIC values for one-compartment and two-compartment fitting of plasma lipid and DB-67 disposition

Experiment #	Cholesterol Content (mole%)	Particle Size (nm)	Lipid Dose (mg/kg)	DB-67 Dose (mg/kg)	AIC for Lipid Disposition		AIC for DB-67 Disposition	
					One-compartment	Two-compartment	One-compartment	Two-compartment
LP-5	0	121±18	234.5	1.34	6.25	10.87	6.17	7.56
LP-3	0	179±21	255.9	1.36	28.96	16.85	9.36	12.43
LP-2	40	121±17	235.8	0.24	7.76	5.67	18.60	22.10
LP-4	40	187±23	240.1	1.07	37.42	28.75	13.50	15.07
LP-7	0	103±11	63.6	0.30	33.07	36.74	21.83	26.39
LP-6	0	115±16	703.9	3.35	30.70	29.30	39.49	24.60

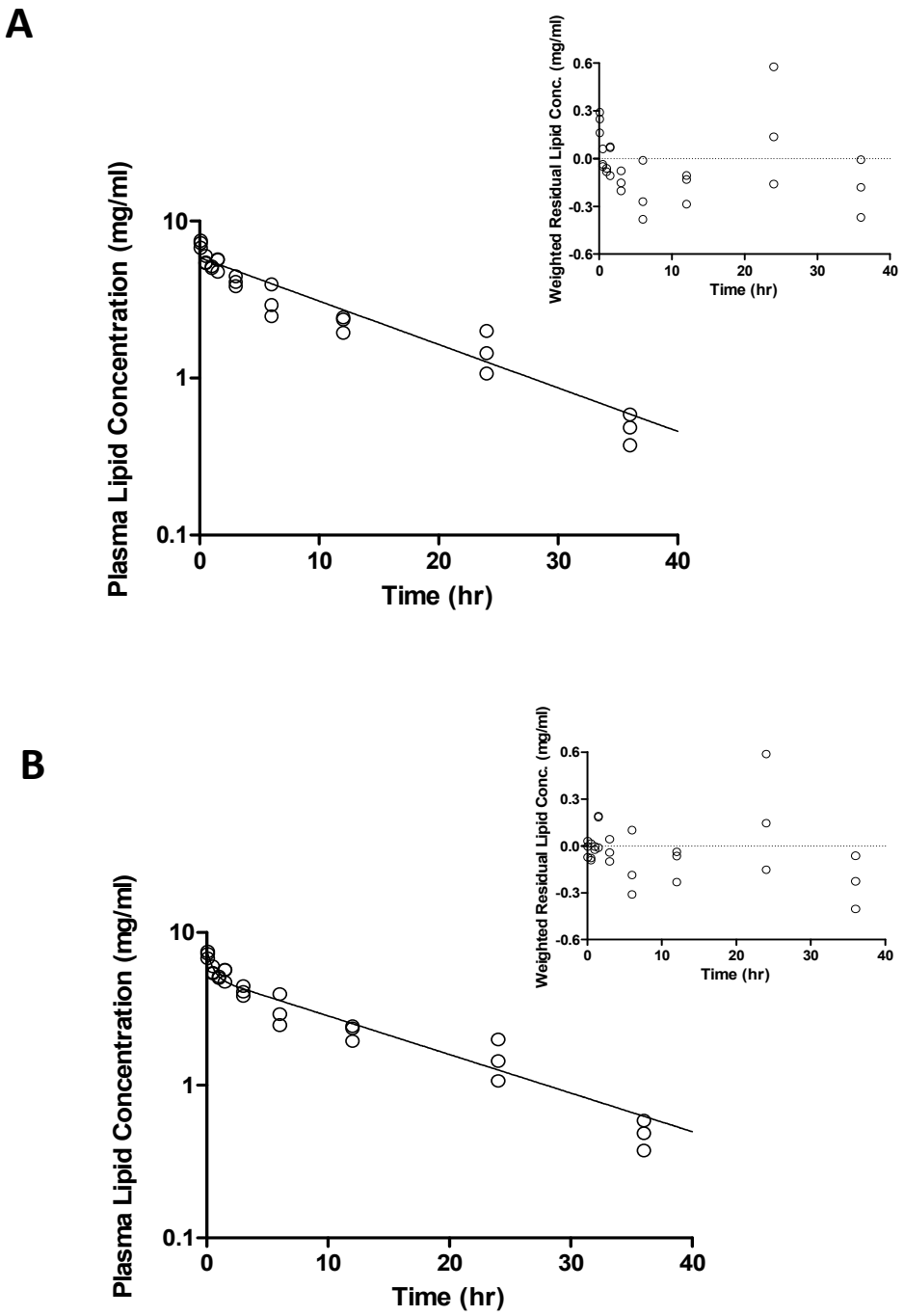

Figure 7. 1 Plasma lipid concentration profiles for cholesterol-containing (40%, molar ratio) liposomes with particle size of 121±17 nm (LP-2).
One-compartment (A) and two-compartment model (B) were fitted to the data respectively. The associated weighted residual plots are shown in the right upper corner. The Lipid and DB-67 doses are shown in Table 7.4. Open circles represent observed values and solid lines represent predicted values.

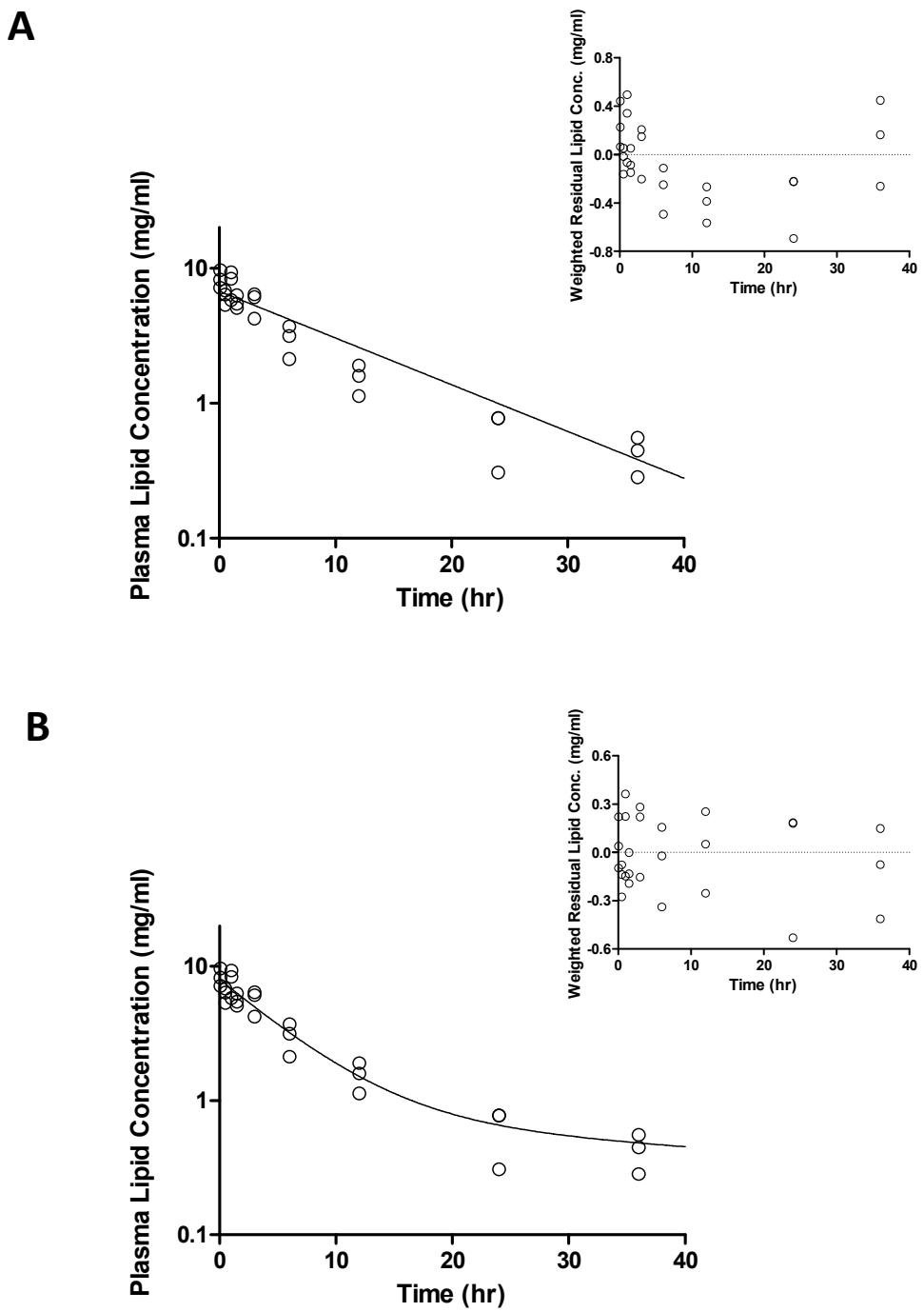

Figure 7. 2 Plasma lipid concentration profiles for cholesterol-free liposomes with particle size of 179±21 nm (LP-3).
One-compartment (A) and two-compartment model (B) were fitted to the data respectively. The associated weighted residual plots are shown in the right upper corner. The Lipid and DB-67 doses are shown in Table 7.4. Open circles represent observed values and solid lines represent predicted values.

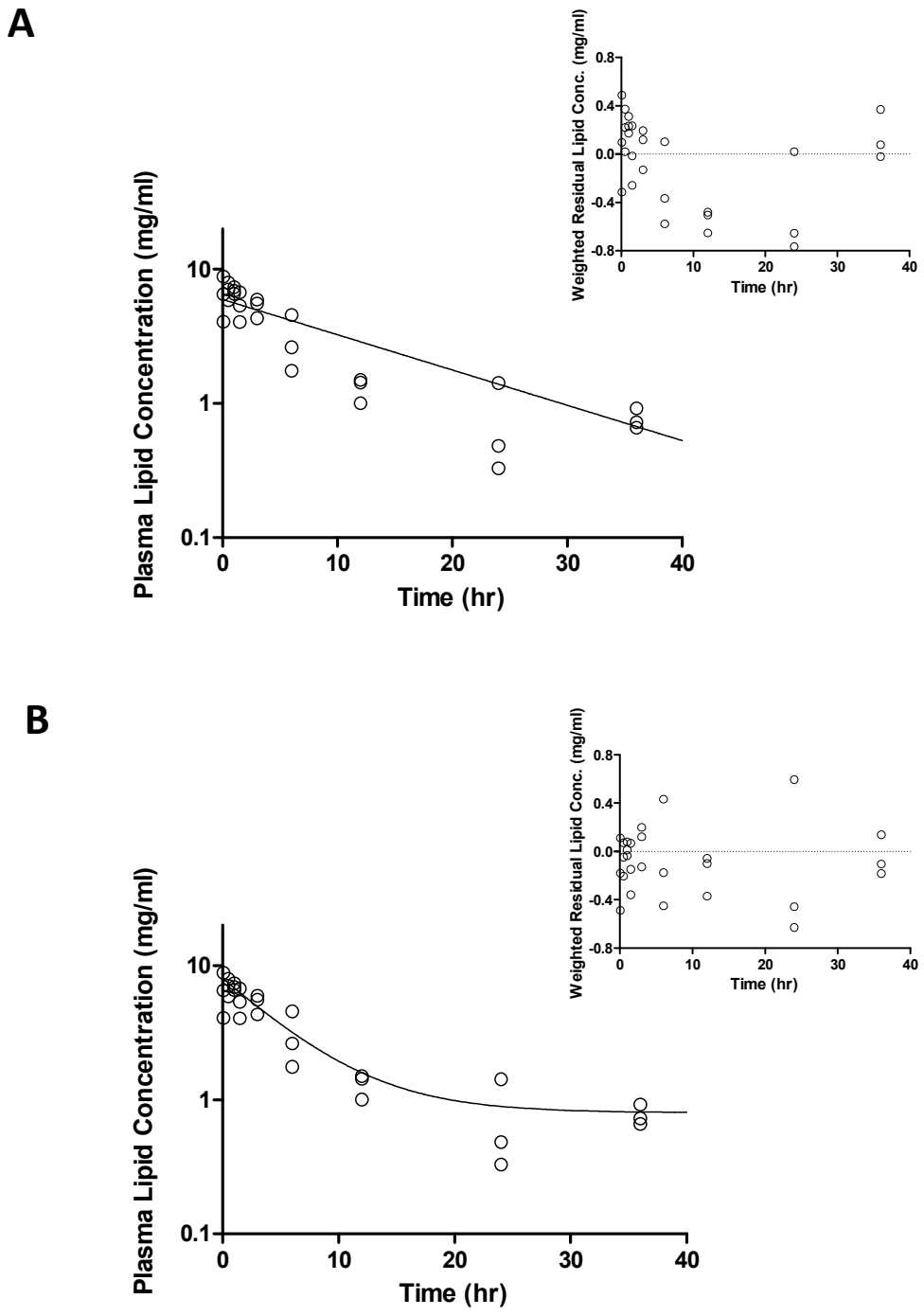

Figure 7. 3 Plasma lipid concentration profiles for cholesterol-containing (40%, molar ratio) liposomes with particle size of 187±23 nm (LP-4).
One-compartment (A) and two-compartment model (B) were fitted to the data respectively. The associated weighted residual plots are shown in the right upper corner. The Lipid and DB-67 doses are shown in Table 7.4. Open circles represent observed values and solid lines represent predicted values.

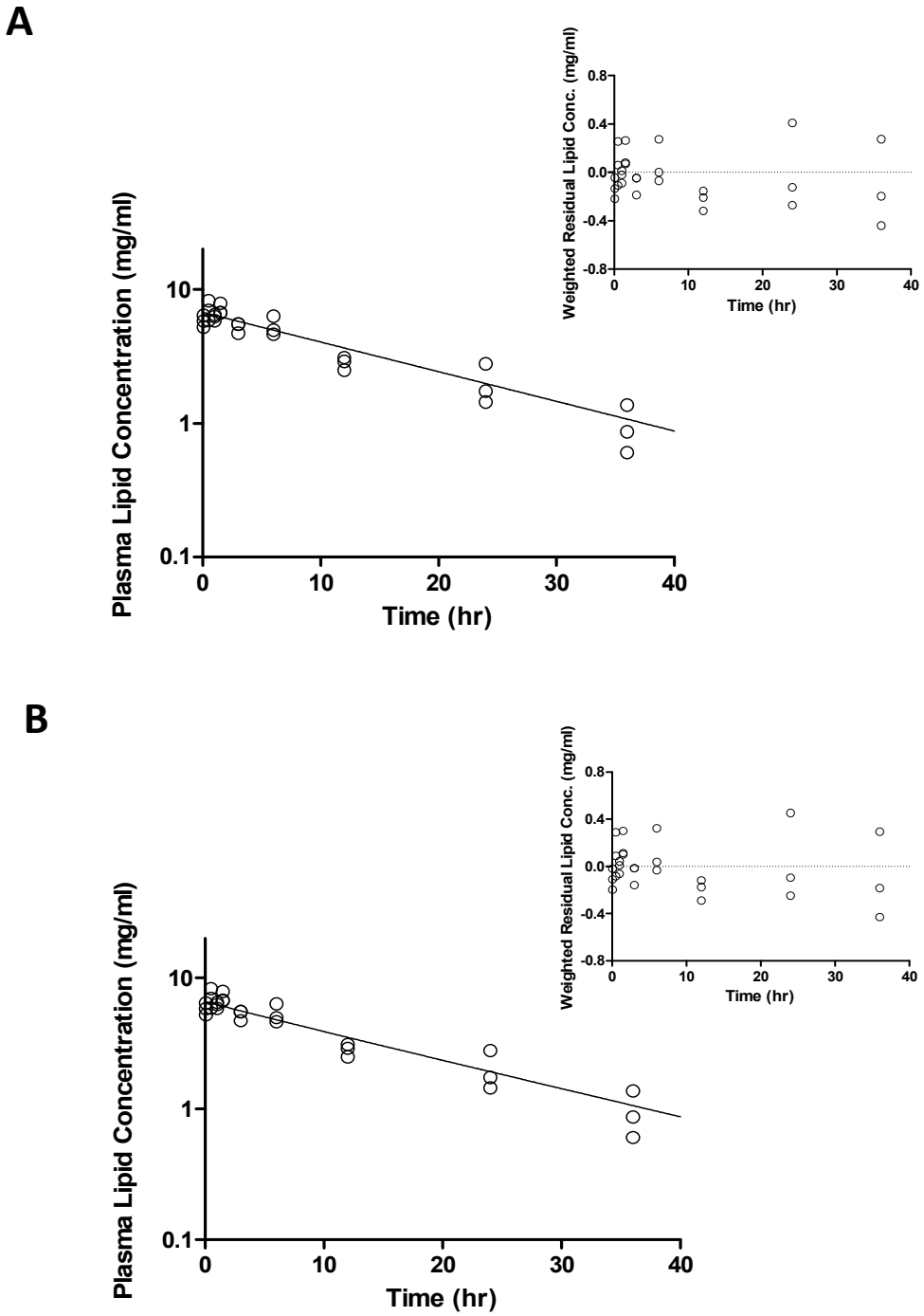

Figure 7. 4 Plasma lipid concentration profiles for cholesterol-free liposomes with particle size of 121±18 nm (LP-5).

One-compartment (A) and two-compartment model (B) were fitted to the data respectively. The associated weighted residual plots are shown in the right upper corner. The Lipid and DB-67 doses are shown in Table 7.4. Open circles represent observed values and solid lines represent predicted values.

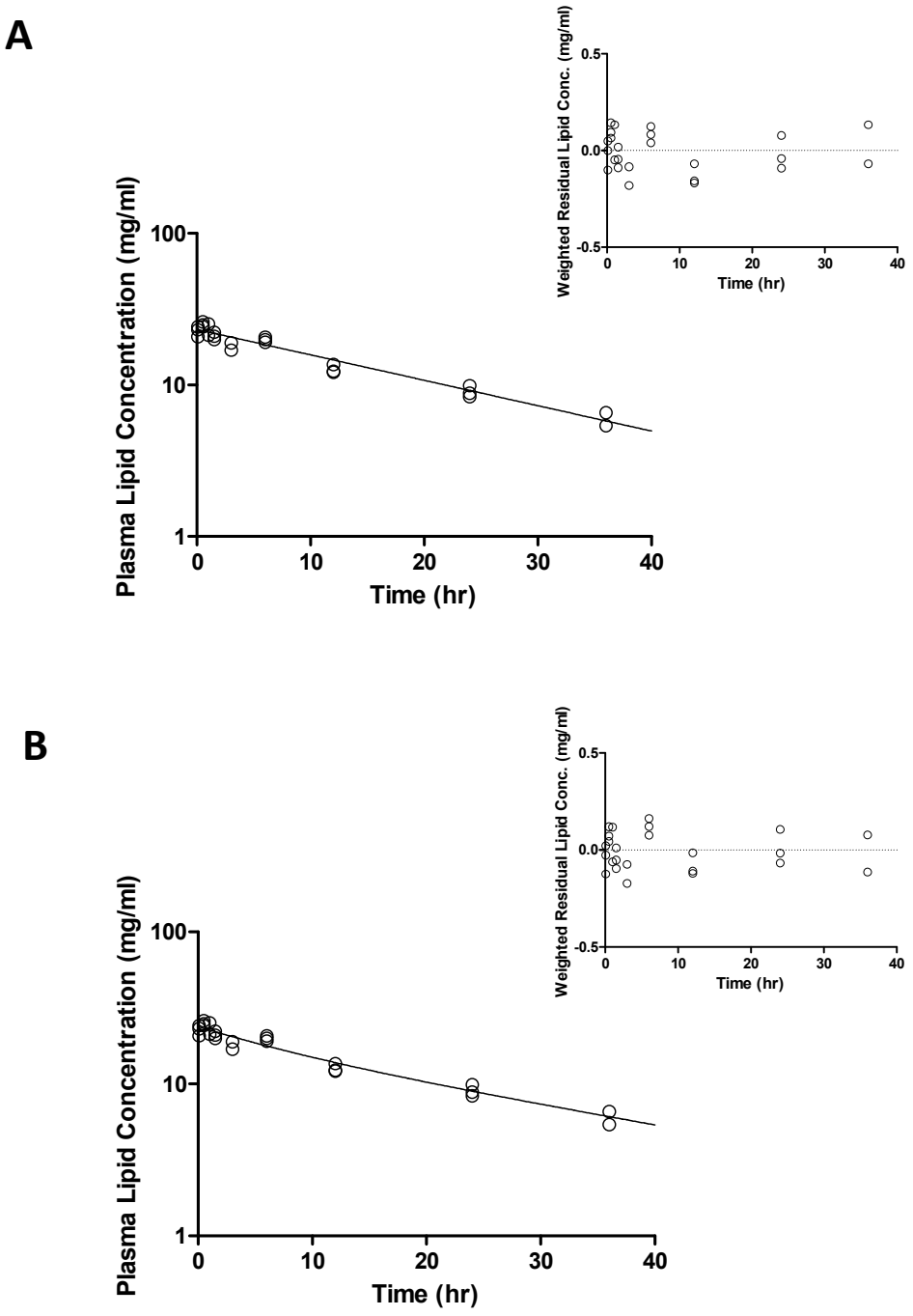

Figure 7. 5 Plasma lipid concentration profiles for cholesterol-free liposomes with particle size of 115±16 nm at the lipid dose of 704 mg/kg (LP-6).
One-compartment (A) and two-compartment model (B) were fitted to the data respectively. The associated weighted residual plots are shown in the right upper corner. DB-67 doses are shown in Table 7.4. Open circles represent observed values and solid lines represent predicted values.

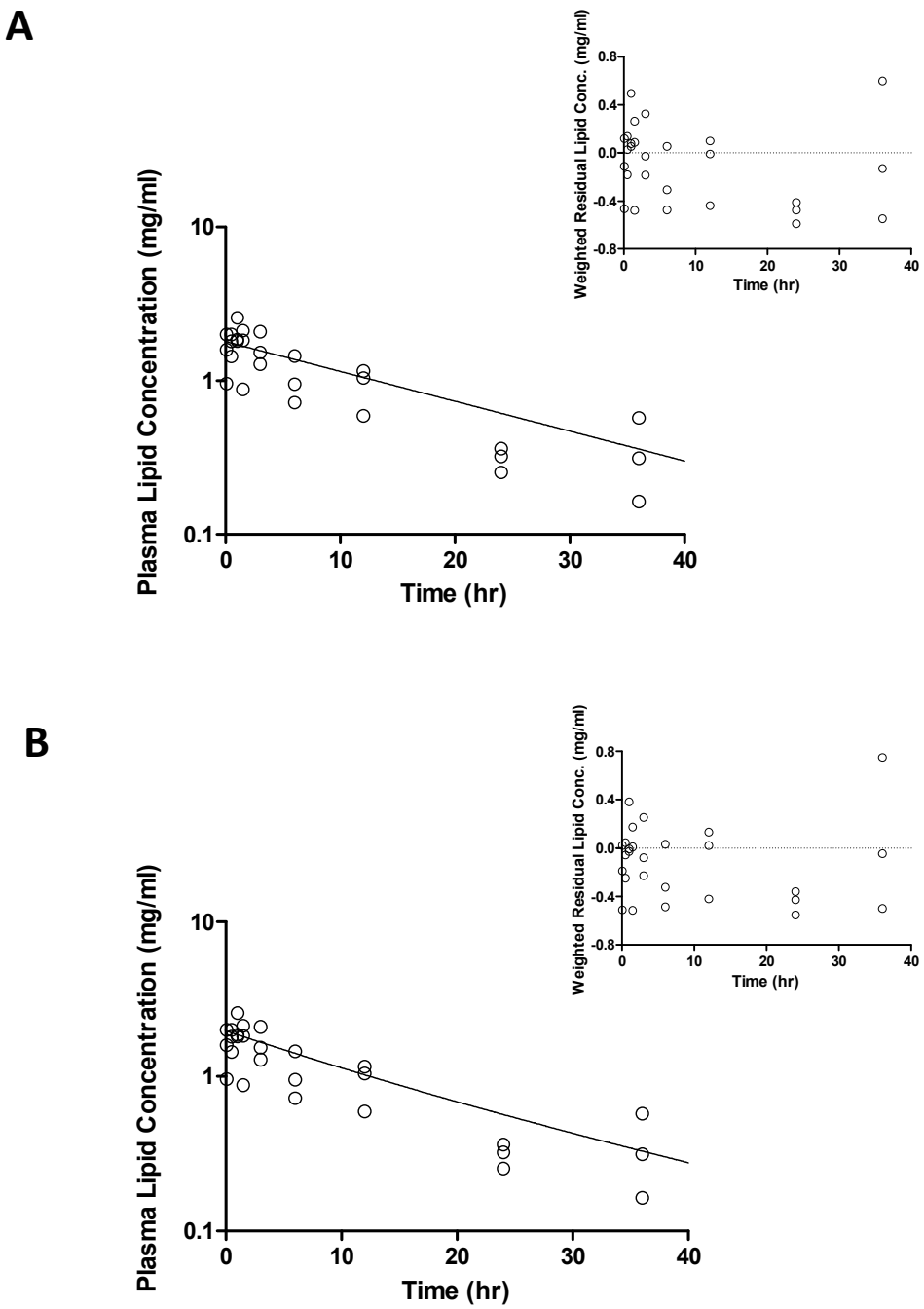

Figure 7. 6 Plasma lipid concentration profiles for cholesterol-free liposomes with particle size of 103±11 nm at the lipid dose of 64 mg/kg (LP-7).
One-compartment (A) and two-compartment model (B) were fitted to the data respectively. The associated weighted residual plots are shown in the right upper corner. DB-67 doses are shown in Table 7.4. Open circles represent observed values and solid lines represent predicted values.

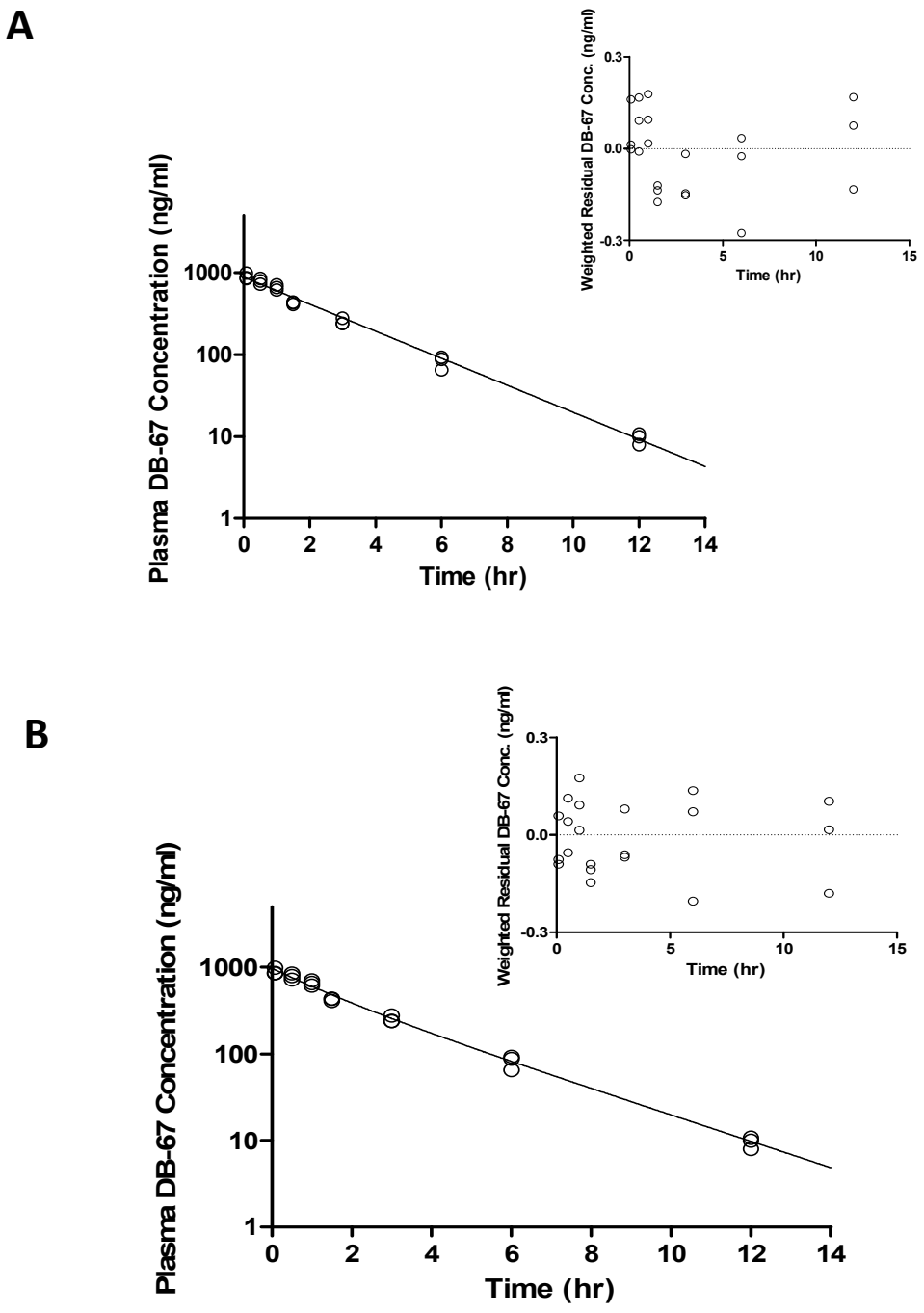

Figure 7. 7 Plasma DB-67 concentration profiles (total of carboxylate and lactone) for cholesterol-containing (40%, molar ratio) liposomes with particle size of 121±17 nm (LP-2).
One-compartment (A) and two-compartment model (B) were fitted to the data respectively. The associated weighted residual plots are shown in the right upper corner. The Lipid and DB-67 doses are shown in Table 7.4. Open circles represent observed values and solid lines represent predicted values.

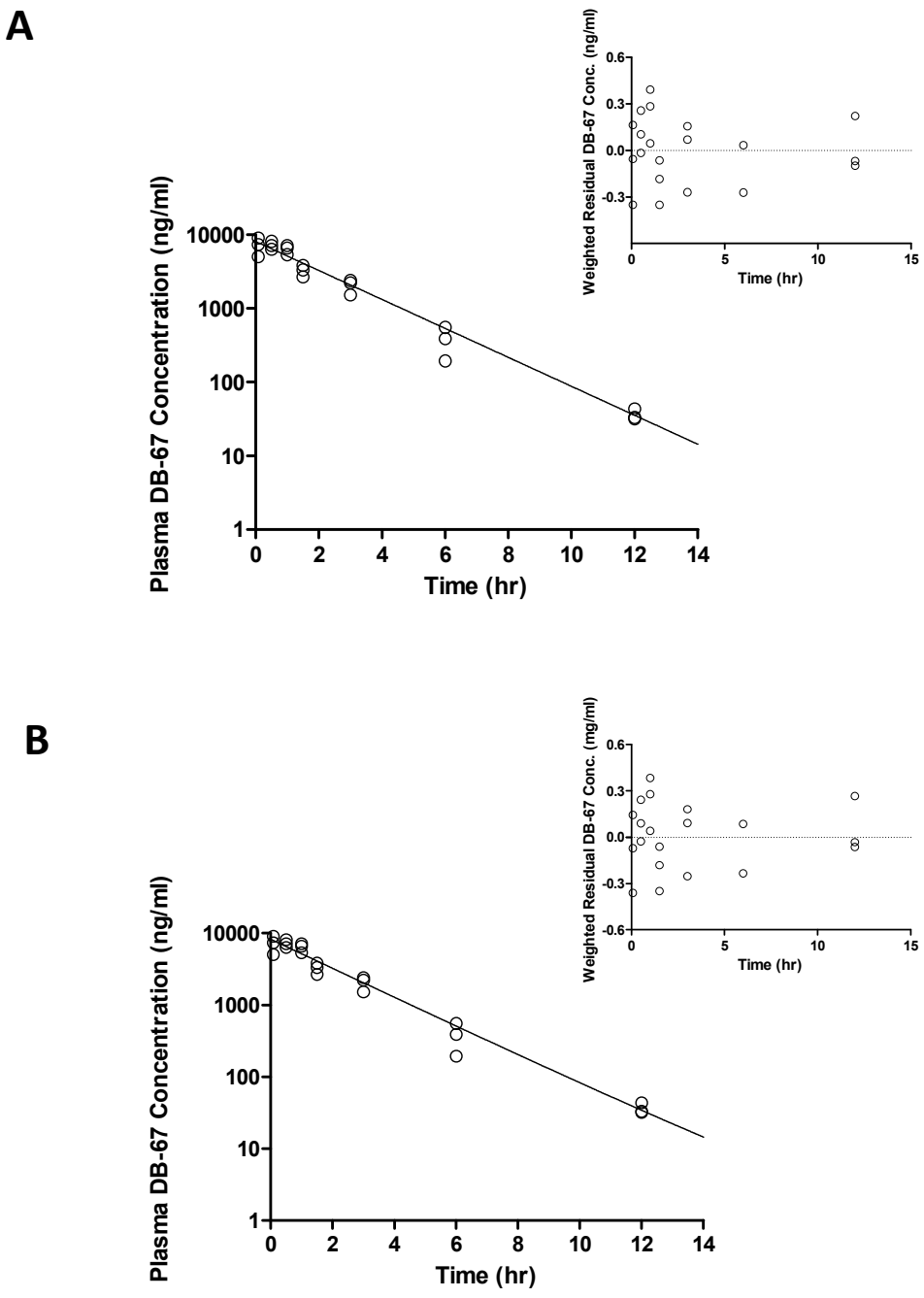

Figure 7. 8 Plasma DB-67 concentration (total of carboxylate and lactone) profiles for cholesterol-free liposomes with particle size of 179±21 nm (LP-3).
One-compartment (A) and two-compartment model (B) were fitted to the data respectively. The associated weighted residual plots are shown in the right upper corner. The Lipid and DB-67 doses are shown in Table 7.4. Open circles represent observed values and solid lines represent predicted values.

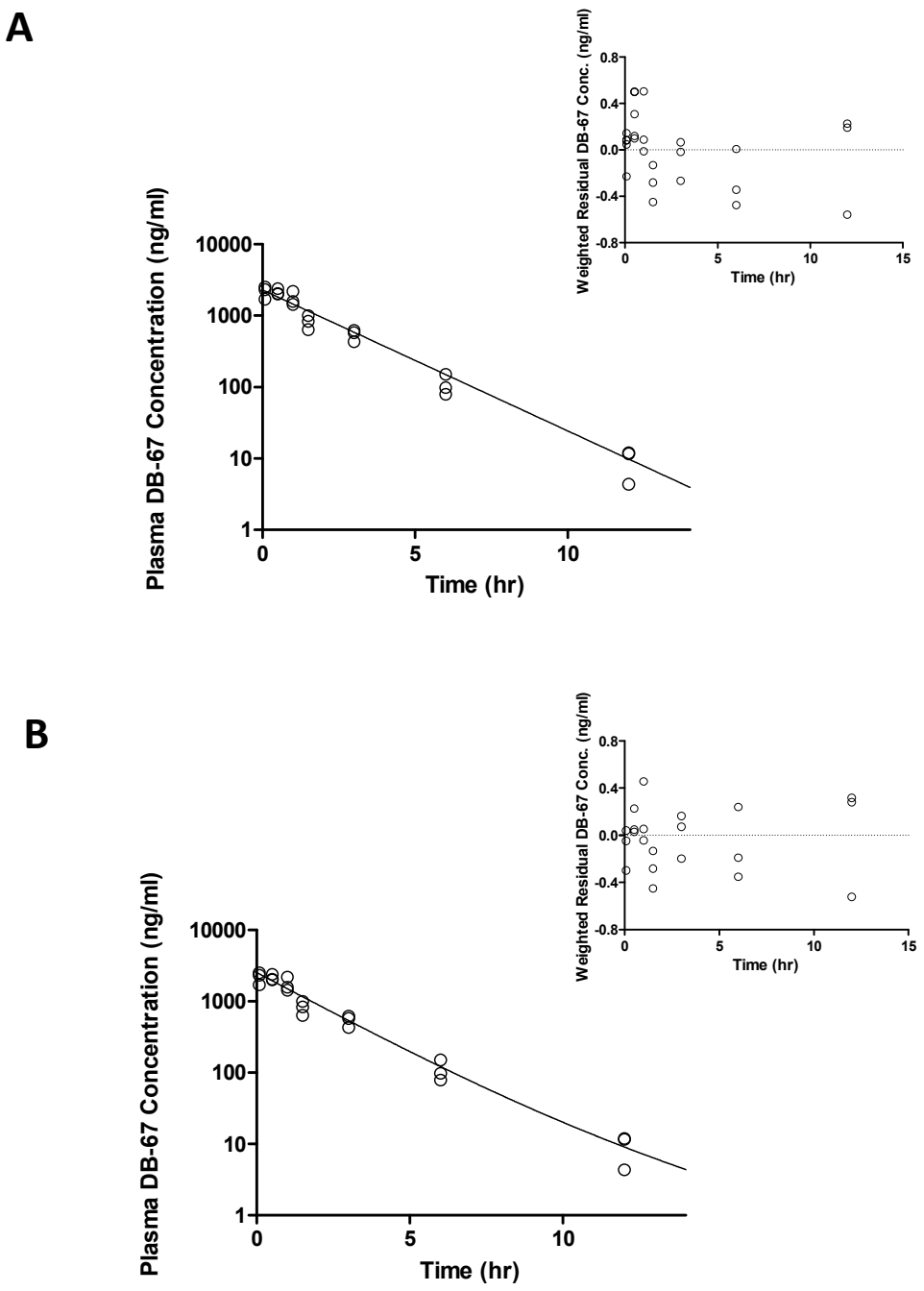

Figure 7. 9 Plasma DB-67 concentration profiles (total of carboxylate and lactone) for cholesterol-containing (40%, molar ratio) liposomes with particle size of 187±23 nm (LP-4).
One-compartment (A) and two-compartment model (B) were fitted to the data respectively. The associated weighted residual plots are shown in the right upper corner. The Lipid and DB-67 doses are shown in Table 7.4. Open circles represent observed values and solid lines represent predicted values.

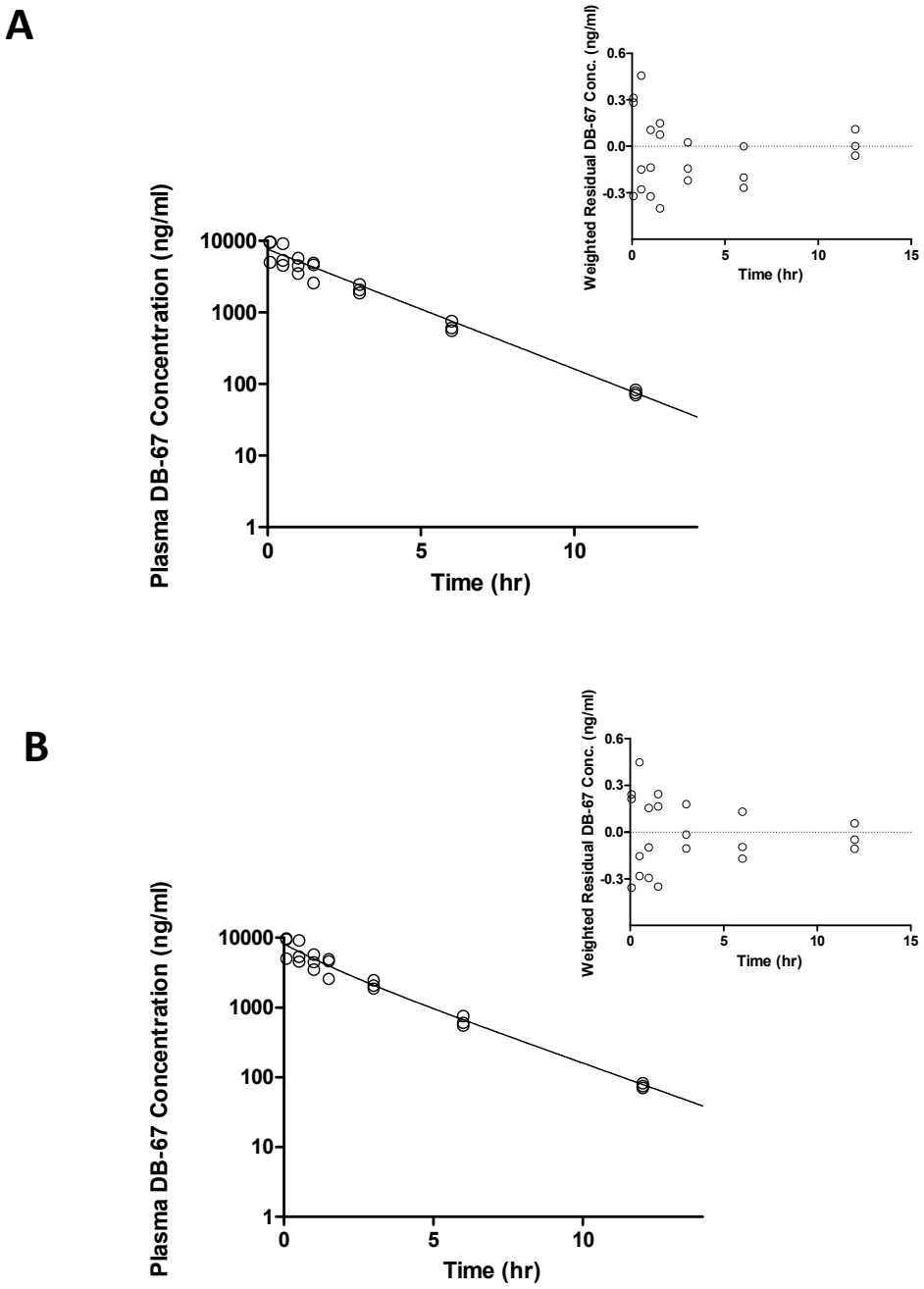

Figure 7. 10 Plasma DB-67 concentration (total of carboxylate and lactone) profiles for cholesterol-free liposomes with particle size of 121±18 nm (LP-5).
One-compartment (A) and two-compartment model (B) were fitted to the data respectively. The associated weighted residual plots are shown in the right upper corner. The Lipid and DB-67 doses are shown in Table 7.4. Open circles represent observed values and solid lines represent predicted values.

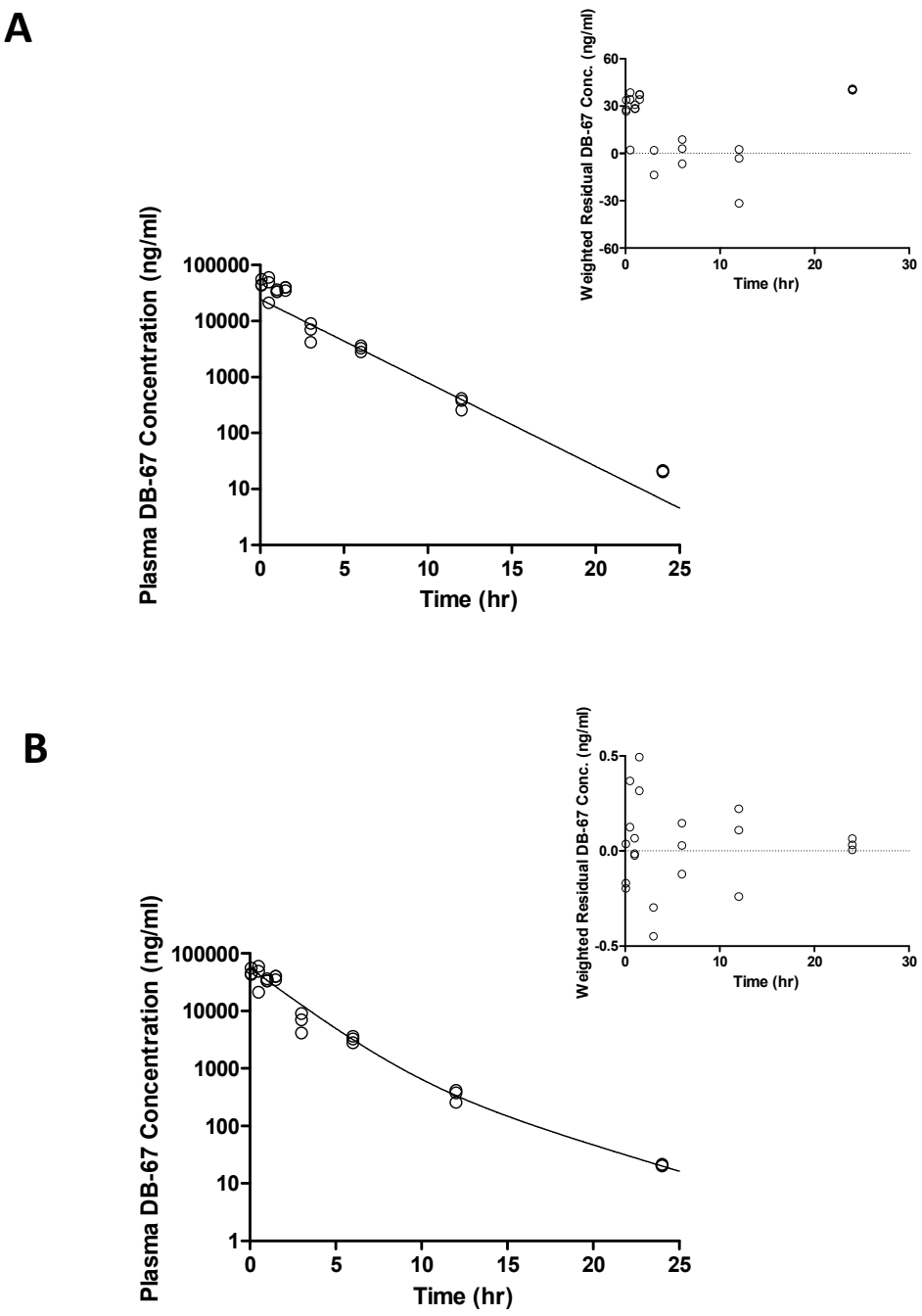

Figure 7. 11 Plasma DB-67 concentration (total of carboxylate and lactone) profiles for cholesterol-free liposomes with particle size of 115±11 nm at the lipid of 704 mg/kg and DB-67 dose of 3.35 mg/kg (LP-6).
One-compartment (A) and two-compartment model (B) were fitted to the data respectively. The associated weighted residual plots are shown in the right upper corner. Open circles represent observed values and solid lines represent predicted values.

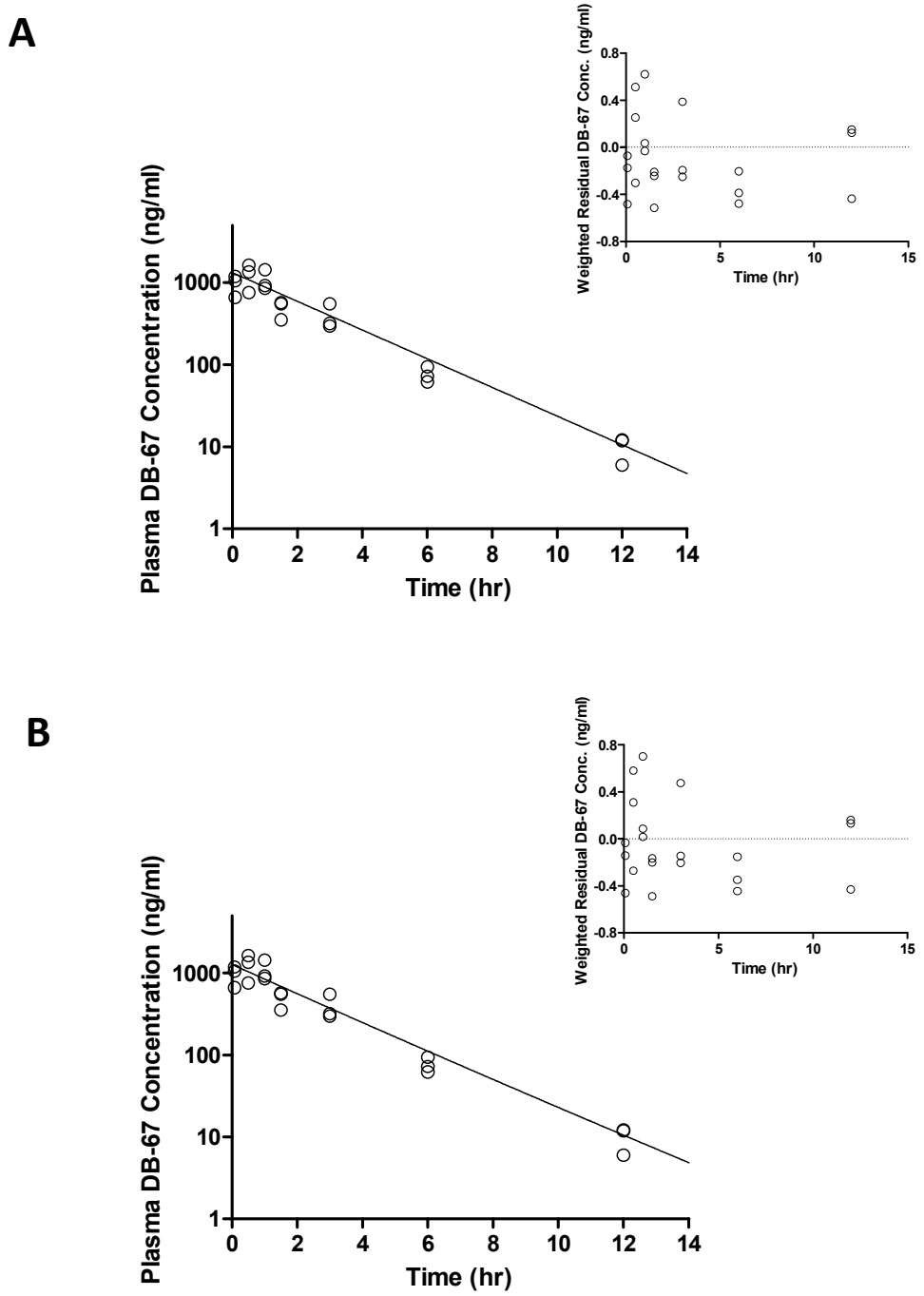

Figure 7. 12 Plasma DB-67 concentration (total of carboxylate and lactone) profiles for cholesterol-free liposomes with particle size of 103 nm at the lipid dose of 64 mg/kg and DB-67 dose of 0.3 mg/kg (LP-7).
One-compartment (A) and two-compartment model (B) were fitted to the data respectively. The associated weighted residual plots are shown in the right upper corner. Open circles represent observed values and solid lines represent predicted values.

Appendix III: Raw Data of Plasma Lipid Concentration and DB-67 Concentration (Carboxylate and Lactone)

Expt #	Time (hr)	Mouse #	Radioactivity (DPM)	Lipid concentration (mg/ml)	DB-67 Carboxylate (ng/ml)	DB-67 Lactone (ng/ml)
LP-2	0.0833	16	50054.33	6.77	340.00	510.75
LP-2	0.0833	17	55579.63	7.52	380.25	609.50
LP-2	0.0833	18	53756.67	7.27	325.50	538.50
LP-2	0.5	13	40420.43	5.47	363.00	431.70
LP-2	0.5	14	39862.3	5.39	309.20	412.00
LP-2	0.5	15	44532.53	6.02	359.60	489.70
LP-2	1	10	37300.67	5.04	301.25	407.65
LP-2	1	11	19043.17	2.57	242.95	368.80
LP-2	1	12	38101.7	5.15	263.25	395.85
LP-2	1.5	16	35125.07	4.75	164.44	246.62
LP-2	1.5	17	42309.7	5.72	104.30	325.84
LP-2	1.5	18	42043.6	5.68	167.20	270.98
LP-2	3	10	33004.43	4.46	111.01	165.72
LP-2	3	11	30312	4.10	97.74	142.85
LP-2	3	12	28529.7	3.86	96.38	142.13
LP-2	6	13	18295.63	2.47	27.53	37.74
LP-2	6	14	29210.97	3.95	37.04	50.78
LP-2	6	15	21594.03	2.92	37.19	55.93
LP-2	12	16	17522	2.37	3.43	4.57
LP-2	12	17	18025.3	2.44	4.06	5.85
LP-2	12	18	14390.5	1.94	4.51	6.25
LP-2	24	13	14792.73	2.00	< 2.50	< 5.00
LP-2	24	14	7895.933	1.07	< 2.50	< 5.00
LP-2	24	15	10666.23	1.447	< 2.50	< 5.00
LP-2	36	10	3584.67	0.487	< 2.50	< 5.00
LP-2	36	11	4340.41	0.59	< 2.50	< 5.00
LP-2	36	12	2762.615	0.37	< 2.50	< 5.00

Note: The shaded numbers were excluded from the data analysis, because less than 20 µl of plasma was collected for scintillation counting.

Expt #	Time (hr)	Mouse #	Radioactivity (DPM)	Lipid concentration (mg/ml)	DB-67 Carboxylate (ng/ml)	DB-67 Lactone (ng/ml)
LP-3	0.0833	25	66761.5	9.673651	4592.00	4504.50
LP-3	0.0833	26	49349.4	7.150661	4197.50	3181.50
LP-3	0.0833	27	56826.7	8.234112	2907.50	2178.00
LP-3	0.6833	19	37025.7	5.364974	4475.50	3654.00
LP-3	0.5	23	44122.3	6.393262	3417.00	2956.00
LP-3	0.5	24	47202.5	6.839578	3859.00	3280.00
LP-3	1	22	40269.2	5.834953	3735.50	2891.75
LP-3	1	20	64331.4	9.321533	3974.00	3199.00
LP-3	1	21	57744.2	8.367057	2822.00	2574.50
LP-3	1.5	25	43558.4	6.311553	1503.50	1173.00
LP-3	1.5	26	35190.9	5.099114	1934.00	1428.50
LP-3	1.5	27	37821.6	5.480299	2188.00	1666.50
LP-3	3	19	29230.1	4.235402	880.25	646.00
LP-3	3	20	42131.3	6.104768	1337.50	1076.25
LP-3	3	21	44280.6	6.416199	1238.70	992.00
LP-3	6	22	21711.5	3.145967	205.40	186.10
LP-3	6	23	14662.4	2.124562	106.70	87.70
LP-3	6	24	25662.1	3.718404	299.46	255.00
LP-3	12	25	11004.4	1.594523	17.20	15.95
LP-3	12	26	13120.6	1.901157	20.98	22.38
LP-3	12	27	7810.14	1.131679	16.78	15.27
LP-3	24	22	5369.37	0.778014	< 2.50	< 5.00
LP-3	24	23	2126.39	0.308111	< 2.50	< 5.00
LP-3	24	24	5348.33	0.774966	< 2.50	< 5.00
LP-3	36	19	1956.68	0.28352	< 2.50	< 5.00
LP-3	36	20	3832.15	0.555273	< 2.50	< 5.00
LP-3	36	21	3083.29	0.446765	< 2.50	< 5.00

Expt #	Time (hr)	Mouse #	Radioactivity (DPM)	Lipid concentration (mg/ml)	DB-67 Carboxylate (ng/ml)	DB-67 Lactone (ng/ml)
LP-4	0.0833	34	48367.7	6.520925	1669.50	645.25
LP-4	0.0833	35	65571.1	8.840284	1823.75	701.25
LP-4	0.0833	36	30227.8	4.075307	1227.50	476.25
LP-4	0.5	31	52428.8	7.068441	1391.80	654.00
LP-4	0.5	32	43830.1	5.909166	1652.80	740.00
LP-4	0.5	33	58957.2	7.948599	1403.00	607.00
LP-4	1	28	54692.7	7.37366	1512.80	677.30
LP-4	1	29	48941.9	6.598338	999.80	438.00
LP-4	1	30	51345.1	6.922337	1091.80	491.40
LP-4	1.5	34	39856.5	5.373446	595.50	238.05
LP-4	1.5	35	49924.2	6.730772	715.00	291.95
LP-4	1.5	36	30019.9	4.047278	454.50	184.30
LP-4	3	28	44141.3	5.951122	439.50	185.45
LP-4	3	29	32126.3	4.331262	306.10	124.30
LP-4	3	30	41302.8	5.568436	405.05	170.90
LP-4	6	31	19529.9	2.633018	51.81	27.02
LP-4	6	32	33907.4	4.57139	100.56	50.13
LP-4	6	33	13024.5	1.755961	67.12	31.33
LP-4	12	34	10647.9	1.435548	8.11	3.52
LP-4	12	35	11154.8	1.503888	7.77	4.19
LP-4	12	36	7448.83	1.00425	4.34	< 5.00
LP-4	24	31	3594.56	0.484618	< 2.50	< 5.00
LP-4	24	32	10566.5	1.424574	< 2.50	< 5.00
LP-4	24	33	2447.22	0.329934	< 2.50	< 5.00
LP-4	36	28	6851.85	0.923765	< 2.50	< 5.00
LP-4	36	29	4908.4	0.66175	< 2.50	< 5.00
LP-4	36	30	5395.16	0.727374	< 2.50	< 5.00

Expt #	Time (hr)	Mouse #	Radioactivity (DPM)	Lipid concentration (mg/ml)	DB-67 Carboxylate (ng/ml)	DB-67 Lactone (ng/ml)
LP-5	0.0833	43	46703.45	6.422776	6915.50	2796.50
LP-5	0.0833	44	39884.35	5.246911	3625.00	1401.00
LP-5	0.0833	45	44416.1	5.823845	6756.00	2729.50
LP-5	0.5	40	42480.75	5.865556	3798.25	1566.00
LP-5	0.5	41	50946.2	6.966093	3213.00	1337.50
LP-5	0.5	42	60005.65	8.248725	5394.50	3779.50
LP-5	1	37	46933.05	6.496248	4226.75	1521.50
LP-5	1	38	45640	6.284752	2139.75	1373.25
LP-5	1	39	42754.6	5.838697	3243.00	1244.25
LP-5	1.5	43	29789.25	6.748423	3731.25	1195.00
LP-5	1.5	44	30597.55	6.681367	1955.50	615.00
LP-5	1.5	45	38893.05	7.889997	3479.00	1129.00
LP-5	3	37	40204.2	5.516922	1597.00	462.90
LP-5	3	38	39968.45	5.511408	1844.00	620.75
LP-5	3	39	34129.15	4.705072	1411.40	460.50
LP-5	6	40	33610.6	4.626987	407.10	147.20
LP-5	6	41	36034.9	4.967052	441.00	163.60
LP-5	6	42	46088.3	6.327466	551.10	205.20
LP-5	12	43	21085.35	2.898026	61.95	21.22
LP-5	12	44	18162.2	2.494727	53.53	16.91
LP-5	12	45	22486.65	3.09108	57.38	17.60
LP-5	24	40	30459.25	1.443656	< 2.50	< 5.00
LP-5	24	41	30478.65	1.738491	< 2.50	< 5.00
LP-5	24	42	38957	2.790538	2.99	< 5.00
LP-5	36	37	9898.145	1.370118	< 2.50	< 5.00
LP-5	36	38	6206	0.863244	< 2.50	< 5.00
LP-5	36	39	4393.815	0.603769	< 2.50	< 5.00

Expt #	Time (hr)	Mouse #	Radioactivity (DPM)	Lipid concentration (mg/ml)	DB-67 Carboxylate (ng/ml)	DB-67 Lactone (ng/ml)
LP-6	0.0833	52	59487	24.25703	31410.00	13555.00
LP-6	0.0833	53	56690.4	23.11666	29375.00	14065.00
LP-6	0.0833	54	51023.1	20.8057	38485.00	17670.00
LP-6	0.5	49	63818	26.02308	36815.00	12585.00
LP-6	0.5	50	61045.8	24.89266	14970.00	6335.00
LP-6	0.5	51	59457.3	24.24492	41255.00	18820.00
LP-6	1	46	62035.1	25.29607	25510.00	7890.00
LP-6	1	47	52115.5	21.25115	26770.00	9690.00
LP-6	1	48	37775	15.40352	25382.50	8327.50
LP-6	1.5	52	54677.2	22.29574	30260.00	9920.00
LP-6	1.5	53	51277.4	20.9094	29747.50	10102.50
LP-6	1.5	54	48961.7	19.96513	26292.50	8807.50
LP-6	3	46	46475	18.95112	7051.00	1953.00
LP-6	3	47	41556.2	16.94538	5553.50	1505.50
LP-6	3	48	29734	12.12464	3150.00	998.00
LP-6	6	49	50752.7	20.69544	2450.50	826.75
LP-6	6	50	48918.7	19.94759	2687.00	962.50
LP-6	6	51	46946.8	19.14351	2125.00	668.50
LP-6	12	52	33390.5	13.61565	281.94	94.02
LP-6	12	53	30202.7	12.31576	299.08	114.98
LP-6	12	54	29822.3	12.16065	189.80	67.70
LP-6	24	49	21630.3	8.820193	15.52	5.24
LP-6	24	50	24325.8	9.919338	15.37	6.03
LP-6	24	51	20517.2	8.366304	14.93	5.28
LP-6	36	46	16090.8	6.56135	< 2.50	< 5.00
LP-6	36	47	13228.3	5.394107	< 2.50	< 5.00
LP-6	36	48	2644.43	1.07832	< 2.50	< 5.00

Note: The shaded numbers were excluded from the data analysis, because less than 20 μl of plasma was collected for scintillation counting.

Expt #	Time (hr)	Mouse #	Radioactivity (DPM)	Lipid concentration (mg/ml)	DB-67 Carboxylate (ng/ml)	DB-67 Lactone (ng/ml)
LP-7	0.0833	61	21422.3	0.960144	518.75	145.00
LP-7	0.0833	62	35597.5	1.595474	903.40	288.00
LP-7	0.0833	63	44847.4	2.010052	790.30	268.40
LP-7	0.5	58	40381	1.809869	1237.10	402.10
LP-7	0.5	59	44742.2	2.005337	1040.60	318.40
LP-7	0.5	60	32206.8	1.443503	596.10	161.50
LP-7	1	55	57495.7	2.576947	1215.40	220.80
LP-7	1	56	40493.9	1.814929	791.50	125.50
LP-7	1	57	41387.9	1.854998	745.70	113.90
LP-7	1.5	61	19629	0.879768	321.60	30.70
LP-7	1.5	62	40857.6	1.83123	482.40	67.55
LP-7	1.5	63	47495.3	2.128731	505.95	67.30
LP-7	3	55	46615.6	2.089303	497.90	52.15
LP-7	3	56	34192.1	1.532484	290.60	28.75
LP-7	3	57	28681.3	1.285491	269.80	27.20
LP-7	6	58	32427.2	1.453381	80.31	14.20
LP-7	6	59	16154.7	0.724051	62.34	10.36
LP-7	6	60	21302.6	0.954779	53.22	8.79
LP-7	12	61	13228.3	0.59289	5.99	< 5.00
LP-7	12	62	25845.1	1.158373	11.89	< 5.00
LP-7	12	63	23313.1	1.044889	12.18	< 5.00
LP-7	24	58	8093.75	0.36276	< 2.50	< 5.00
LP-7	24	59	7217.55	0.323489	< 2.50	< 5.00
LP-7	24	60	5656.85	0.253539	< 2.50	< 5.00
LP-7	36	55	12833.3	0.575186	< 2.50	< 5.00
LP-7	36	56	6993.26	0.313437	< 2.50	< 5.00
LP-7	36	57	3657.24	0.163917	< 2.50	< 5.00

Bibliography

Adane ED, Liu Z, Xiang TX, Anderson BD, Leggas M. 2010. Factors affecting the in vivo lactone stability and systemic clearance of the lipophilic camptothecin analogue AR-67. Pharm Res 27(7):1416-25.

Agresti A. 1990. Asymptotic Theory For Parametric Models. Categorical Data Analysis. New York: Wiley-Interscience Publication. p 419-423.

Allen TM, Cheng WW, Hare JI, Laginha KM. 2006. Pharmacokinetics and pharmacodynamics of lipidic nano-particles in cancer. Anticancer Agents Med Chem 6(6):513-23.

Allen TM, Chonn A. 1987. Large unilamellar liposomes with low uptake into the reticuloendothelial system. FEBS Letters 223(1):42-46.

Allen TM, Hansen C. 1991. Pharmacokinetics of stealth versus conventional liposomes: effect of dose. Biochimica et Biophysica Acta (BBA) - Biomembranes 1068(2):133-141.

Allen TM, Hansen CB, de Menezes DEL. 1995. Pharmacokinetics of long-circulating liposomes. Advanced Drug Delivery Reviews 16(2-3):267-284.

Allen TM, Murray L, MacKeigan S, Shah M. 1984. Chronic liposome administration in mice: effects on reticuloendothelial function and tissue distribution. J Pharmacol Exp Ther 229(1):267-75.

Arnold SM, Rinehart JJ, Tsakalozou E, Eckardt JR, Fields SZ, Shelton BJ, DeSimone PA, Kee BK, Moscow JA, Leggas M. 2010. A Phase I Study of 7-t-Butyldimethylsilyl-10-Hydroxycamptothecin in Adult Patients with Refractory or Metastatic Solid Malignancies. Clinical Cancer Research 16(2):673-680.

Bailer AJ. 1988. Testing for the equality of area under the curves when using destructive measurement techniques. J Pharmacokinet Biopharm 16(3):303-9.

Bence AK, Mattingly CA, Burke TG, Adams VR. 2004. The effect of DB-67, a lipophilic camptothecin derivative, on topoisomerase I levels in non-small-cell lung cancer cells. Cancer Chemotherapy and Pharmacology 54(4):354-360.

Boiardi A, Pozzi A, Salmaggi A, Eoli M, Zucchetti M, Silvani A. 1999. Safety and potential effectiveness of daunorubicin-containing liposomes in patients with advanced recurrent malignant CNS tumors. Cancer Chemother Pharmacol 43(2):178-9.

Bom D, Curran DP, Chavan AJ, Kruszewski S, Zimmer SG, Fraley KA, Burke TG. 1999. Novel A,B,E-Ring-Modified Camptothecins Displaying High Lipophilicity and Markedly Improved Human Blood Stabilities. Journal of Medicinal Chemistry 42(16):3018-3022.

Bom D, Curran DP, Kruszewski S, Zimmer SG, Thompson Strode J, Kohlhagen G, Du W, Chavan AJ, Fraley KA, Bingcang AL and others. 2000. The Novel Silatecan 7-tert-Butyldimethylsilyl-10-hydroxycamptothecin Displays High Lipophilicity, Improved Human Blood Stability, and Potent Anticancer Activity. Journal of Medicinal Chemistry 43(21):3970-3980.

Bom D, Curran DP, Zhang J, Zimmer SG, Bevins R, Kruszewski S, Howe JN, Bingcang A, Latus LJ, Burke TG. 2001. The highly lipophilic DNA topoisomerase I inhibitor DB-67 displays elevated lactone levels in human blood and potent anticancer activity. Journal of Controlled Release 74(1-3):325-333.

Burke TG, Bom D. 2000. Campthotecin Design and Delivery Approaches for Elevating Anti-Topoisomerase I Activities in Vivo. Annals of the New York Academy of Sciences 922(THE CAMPTOTHECINS: UNFOLDING THEIR ANTICANCER POTENTIAL):36-45.

Burris HA, 3rd, Hanauske AR, Johnson RK, Marshall MH, Kuhn JG, Hilsenbeck SG, Von Hoff DD. 1992. Activity of topotecan, a new topoisomerase I inhibitor, against human tumor colony-forming units in vitro. J Natl Cancer Inst 84(23):1816-20.

Charrois GJ, Allen TM. 2003. Rate of biodistribution of STEALTH liposomes to tumor and skin: influence of liposome diameter and implications for toxicity and therapeutic activity. Biochim Biophys Acta 1609(1):102-8.

Cutnell J, Johnson K. 1998. Mass Densities of Common Substances. Physics. 4th ed: Wiley. p 308.

Damen J, Regts J, Scherphof G. 1981. Transfer and exchange of phospholipid between small unilamellar liposomes and rat plasma high density lipoproteins. Dependence on cholesterol content and phospholipid composition. Biochim Biophys Acta 665(3):538-45.

Dancey J, Eisenhauer EA. 1996. Current perspectives on camptothecins in cancer treatment. Br J Cancer 74(3):327-38.

Dos Santos N, Mayer LD, Abraham SA, Gallagher RC, Cox KAK, Tardi PG, Bally MB. 2002. Improved retention of idarubicin after intravenous injection obtained for cholesterol-free liposomes. Biochimica et Biophysica Acta (BBA) - Biomembranes 1561(2):188-201.

Drummond DC, Meyer O, Hong K, Kirpotin DB, Papahadjopoulos D. 1999. Optimizing Liposomes for Delivery of Chemotherapeutic Agents to Solid Tumors. Pharmacological Reviews 51(4):691-744.

Drummond DC, Noble CO, Guo Z, Hayes ME, Connolly-Ingram C, Gabriel BS, Hann B, Liu B, Park JW, Hong K and others. 2009. Development of a highly stable and targetable nanoliposomal formulation of topotecan. J Control Release 141(1):13-21.

Drummond DC, Noble CO, Hayes ME, Park JW, Kirpotin DB. 2008. Pharmacokinetics and in vivo drug release rates in liposomal nanocarrier development. Journal of Pharmaceutical Sciences 97(11):4696-4740.

Eng WK, Faucette L, Johnson RK, Sternglanz R. 1988. Evidence that DNA topoisomerase I is necessary for the cytotoxic effects of camptothecin. Mol Pharmacol 34(6):755-60.

Forssen EA, Male-Brune R, Adler-Moore JP, Lee MJ, Schmidt PG, Krasieva TB, Shimizu S, Tromberg BJ. 1996. Fluorescence imaging studies for the disposition of daunorubicin liposomes (DaunoXome) within tumor tissue. Cancer Res 56(9):2066-75.

Garcia-Carbonero R, Supko JG. 2002. Current perspectives on the clinical experience, pharmacology, and continued development of the camptothecins. Clin Cancer Res 8(3):641-61.

Georgiadis MS, Russell EK, Gazdar AF, Johnson BE. 1997. Paclitaxel cytotoxicity against human lung cancer cell lines increases with prolonged exposure durations. Clin Cancer Res 3(3):449-54.

Gomi K, Ohno H, Nomura K, Okabe M, Kobayashi K, Niitani H. 1992. Kinetic analysis of combination effect of navelbine (KW-2307) with cisplatin against human lung adenocarcinoma PC-12 cells in culture. Jpn J Cancer Res 83(5):532-9.

Horn J, Jordan SL, Song L, Roberts MJ, Anderson BD, Leggas M. 2006. Validation of an HPLC method for analysis of DB-67 and its water soluble prodrug in mouse plasma. J Chromatogr B Analyt Technol Biomed Life Sci 844(1):15-22.

Hsiang YH, Hertzberg R, Hecht S, Liu LF. 1985. Camptothecin induces protein-linked DNA breaks via mammalian DNA topoisomerase I. J Biol Chem 260(27):14873-8.

Huang SK, Mayhew E, Gilani S, Lasic DD, Martin FJ, Papahadjopoulos D. 1992. Pharmacokinetics and Therapeutics of Sterically Stabilized Liposomes in Mice Bearing C-26 Colon Carcinoma. Cancer Res 52(24):6774-6781.

Hussein MA. 2003. Modifications to therapy for multiple myeloma: pegylated liposomal Doxorubicin in combination with vincristine, reduced-dose dexamethasone, and thalidomide. Oncologist 8 Suppl 3:39-45.

Ishida O, Maruyama K, Sasaki K, Iwatsuru M. 1999. Size-dependent extravasation and interstitial localization of polyethyleneglycol liposomes in solid tumor-bearing mice. Int J Pharm 190(1):49-56.

Joguparthi V. 2007. Physicochemical Approaches to Enhance the Liposomal Loading and Retention of Hydrophobic Weak Acids. Lexington, KY: University of Kentucky. 324 p.

Joguparthi V, Adane ED, Anderson BD, Leggas M. 2008a. Prolonged Liposomal Retention of Highly Lipophilic Camptothecin Analogue AR-67 In Vivo AAPS Annual Meeting and Exposition 2008.

Joguparthi V, Anderson BD. 2008. Liposomal delivery of hydrophobic weak acids: enhancement of drug retention using a high intraliposomal pH. J Pharm Sci 97(1):433-54.

Joguparthi V, Xiang T-X, Anderson BD. 2008b. Liposome transport of hydrophobic drugs: Gel phase lipid bilayer permeability and partitioning of the lactone form of a hydrophobic camptothecin, DB-67. Journal of Pharmaceutical Sciences 97(1):400-420.

Johnston MJW, Semple SC, Klimuk SK, Edwards K, Eisenhardt ML, Leng EC, Karlsson G, Yanko D, Cullis PR. 2006. Therapeutically optimized rates of drug release can be achieved by varying the drug-to-lipid ratio in liposomal vincristine formulations. Biochimica et Biophysica Acta (BBA) - Biomembranes 1758(1):55-64.

Kim ES, Lu C, Khuri FR, Tonda M, Glisson BS, Liu D, Jung M, Hong WK, Herbst RS. 2001. A phase II study of STEALTH cisplatin (SPI-77) in patients with advanced non-small cell lung cancer. Lung Cancer 34(3):427-32.

Kirby C, Clarke J, Gregoriadis G. 1980. Effect of the cholesterol content of small unilamellar liposomes on their stability in vivo and in vitro. Biochem J 186(2):591-8.

Kirpotin DB, Drummond DC, Shao Y, Shalaby MR, Hong K, Nielsen UB, Marks JD, Benz CC, Park JW. 2006. Antibody targeting of long-circulating lipidic nanoparticles does not increase tumor localization but does increase internalization in animal models. Cancer Res 66(13):6732-40.

Klibanov AL, Maruyama K, Beckerleg AM, Torchilin VP, Huang L. 1991. Activity of amphipathic poly(ethylene glycol) 5000 to prolong the circulation time of liposomes depends on the liposome size and is unfavorable for immunoliposome binding to target. Biochim Biophys Acta 1062(2):142-8.

Lasic DD, Martin FJ, Gabizon A, Huang SK, Papahadjopoulos D. 1991. Sterically stabilized liposomes: a hypothesis on the molecular origin of the extended circulation times. Biochim Biophys Acta 1070(1):187-92.

Li X, Hirsh DJ, Cabral-Lilly D, Zirkel A, Gruner SM, Janoff AS, Perkins WR. 1998. Doxorubicin physical state in solution and inside liposomes loaded via a pH gradient. Biochim Biophys Acta 1415(1):23-40.

Litzinger DC, Buiting AM, van Rooijen N, Huang L. 1994. Effect of liposome size on the circulation time and intraorgan distribution of amphipathic poly(ethylene glycol)-containing liposomes. Biochim Biophys Acta 1190(1):99-107.

Lopez-Barcons LA, Zhang J, Siriwitayawan G, Burke TG, Perez-Soler R. 2004. The novel highly lipophilic topoisomerase I inhibitor DB67 is effective in the treatment of liver metastases of murine CT-26 colon carcinoma. Neoplasia 6(5):457-67.

Lum H, Malik AB. 1994. Regulation of vascular endothelial barrier function. Am J Physiol 267(3 Pt 1):L223-41.

Matsumura Y, Maeda H. 1986. A New Concept for Macromolecular Therapeutics in Cancer Chemotherapy: Mechanism of Tumoritropic Accumulation of Proteins and the Antitumor Agent Smancs. Cancer Res 46(12_Part_1):6387-6392.

Mayer LD, Bally MB, Hope MJ, Cullis PR. 1985. Uptake of antineoplastic agents into large unilamellar vesicles in response to a membrane potential. Biochim Biophys Acta 816(2):294-302.

Mayer LD, Tai LC, Bally MB, Mitilenes GN, Ginsberg RS, Cullis PR. 1990. Characterization of liposomal systems containing doxorubicin entrapped in response to pH gradients. Biochim Biophys Acta 1025(2):143-51.

Mayer LD, Tai LC, Ko DS, Masin D, Ginsberg RS, Cullis PR, Bally MB. 1989. Influence of vesicle size, lipid composition, and drug-to-lipid ratio on the biological activity of liposomal doxorubicin in mice. Cancer Res 49(21):5922-30.

Mayhew E, Rustum YM, Szoka F, Papahadjopoulos D. 1979. Role of cholesterol in enhancing the antitumor activity of cytosine arabinoside entrapped in liposomes. Cancer Treat Rep 63(11-12):1923-8.

Messerer CL, Ramsay EC, Waterhouse D, Ng R, Simms EM, Harasym N, Tardi P, Mayer LD, Bally MB. 2004. Liposomal irinotecan: formulation development and therapeutic assessment in murine xenograft models of colorectal cancer. Clin Cancer Res 10(19):6638-49.

Muggia FM. 1997. Clinical efficacy and prospects for use of pegylated liposomal doxorubicin in the treatment of ovarian and breast cancers. Drugs 54 Suppl 4:22-9.

Muggia FM, Burris HA. 1994. Clinical development of topoisomerase-interactive drugs. Adv Pharmacol 29B:1-31.

Nagayasu A, Uchiyama K, Kiwada H. 1999. The size of liposomes: a factor which affects their targeting efficiency to tumors and therapeutic activity of liposomal antitumor drugs. Adv Drug Deliv Rev 40(1-2):75-87.

Nedelman JR, Gibiansky E, Lau DT. 1995. Applying Bailer's method for AUC confidence intervals to sparse sampling. Pharm Res 12(1):124-8.

Ogihara-Umeda I, Kojima S. 1989. Cholesterol enhances the delivery of liposome-encapsulated gallium-67 to tumors. European Journal of Nuclear Medicine and Molecular Imaging 15(9):612-617.

Oja CD, Semple SC, Chonn A, Cullis PR. 1996. Influence of dose on liposome clearance: critical role of blood proteins. Biochim Biophys Acta 1281(1):31-7.

Pollack IF, Erff M, Bom D, Burke TG, Strode JT, Curran DP. 1999. Potent Topoisomerase I Inhibition by Novel Silatecans Eliminates Glioma Proliferation in Vitro and in Vivo. Cancer Res 59(19):4898-4905.

Pommier Y. 2006. Topoisomerase I inhibitors: camptothecins and beyond. Nat Rev Cancer 6(10):789-802.

Pommier Y, Pourquier P, Fan Y, Strumberg D. 1998. Mechanism of action of eukaryotic DNA topoisomerase I and drugs targeted to the enzyme. Biochim Biophys Acta 1400(1-3):83-105.

Semple SC, Chonn A, Cullis PR. 1996. Influence of cholesterol on the association of plasma proteins with liposomes. Biochemistry 35(8):2521-5.

Senior J, Crawley JC, Gregoriadis G. 1985. Tissue distribution of liposomes exhibiting long half-lives in the circulation after intravenous injection. Biochim Biophys Acta 839(1):1-8.

Tardi PG, Gallagher RC, Johnstone S, Harasym N, Webb M, Bally MB, Mayer LD. 2007. Coencapsulation of irinotecan and floxuridine into low cholesterol-containing liposomes that coordinate drug release in vivo. Biochim Biophys Acta 1768(3):678-87.

Vorobiof DA, Rapoport BL, Mahomed R, Karime M. 2003. Phase II study of pegylated liposomal doxorubicin in patients with metastatic malignant melanoma failing standard chemotherapy treatment. Melanoma Res 13(2):201-3.

Waterhouse DN, Tardi PG, Mayer LD, Bally MB. 2001. A comparison of liposomal formulations of doxorubicin with drug administered in free form: changing toxicity profiles. Drug Saf 24(12):903-20.

Woodle MC, Matthay KK, Newman MS, Hidayat JE, Collins LR, Redemann C, Martin FJ, Papahadjopoulos D. 1992. Versatility in lipid compositions showing prolonged circulation with sterically stabilized liposomes. Biochim Biophys Acta 1105(2):193-200.

Xiang TX, Anderson BD. 1997. Permeability of acetic acid across gel and liquid-crystalline lipid bilayers conforms to free-surface-area theory. Biophys J 72(1):223-37.

Ying X, Wen H, Lu WL, Du J, Guo J, Tian W, Men Y, Zhang Y, Li RJ, Yang TY and others. 2009. Dual-targeting daunorubicin liposomes improve the therapeutic efficacy of brain glioma in animals. J Control Release 141(2):183-92.

Zamboni WC, Jung LL, Strychor S, Joseph E, Zamboni BA, Fetterman SA, Sidone BJ, Burke TG, Curran DP, Eiseman JL. 2008. Plasma and tissue disposition of non-liposomal DB-67 and liposomal DB-67 in C.B-17 SCID mice. Invest New Drugs 26(5):399-406.

VITA

Yali Liang was born on July 26, 1976 in Zhangjiakou, Hebei provience, China. She attended the Tongji Medical University at Wuhan, China from 1994 to 1999 and received Bachelor degree in Medicine with highest distinction in June 1999. Yali then continued her graduate training and received a Master of Public Health (M.P.H.) degree at the same university in June 2002. In 2007, she enrolled in the Pharmaceutical Sciences graduate program at the University of Kentucky College of Pharmacy. Yali has held position as a Senior Associate in the Global Pharmacometrics at Pfizer Inc.

Publications:

Yali Liang, Sweta Modi, Markos Leggas, Brad Anderson. The effect of particle size, lipid composition and lipid dose on the *in vitro* drug release and *in vivo* clearance of liposomal DB67. 2009 *(in prep)*.

Yali Liang, Yumin Liu. Quality analysis of drinking water in rural area of Beijing. The Second International Conference on Environmental Concerns Innovative Technologies and Management Options, 2004.

Yali Liang, Binzhi Yin, Xiaozhong Hu. Quick analysis of beta-agonists in urine by Solid Phase Microextraction with headspace derivatization and Gas Chromatography-Mass Spectrometry. Chinese Journal of Analytical Chemistry, 2003; 31(3):326-328.

Dongli Wang, Yali Liang. Determination of Microcystins (MCYST) in water. Chinese Journal of Public Health, 2003; 19 (8): 992-993.

Dongli Wang, Yali Liang. Determination of Chloroethylene by Gas Chromatography (GC) in different environmental mediums. Chinese Journal of Health Laboratory Technology, 2003; 13 (5): 626-627.

Dongying Xu, Yali Liang. Flowing-sampling system for solid phase microextraction in situ. Chinese Journal of Analytical Chemistry, 2002; 30 (11): 1394-1398.

Zhiwei Liu, Yikai Zhou, Yali liang. Luminol/H_2O_2 chemiluminescence detector for the analysis of nitrite in water samples. Chinese Journal of Analytical Chemistry, 2001; 30（5）：632.